To the Graduate Council:

I am submitting herewith a thesis written by Shawn C. Dancik entitled "Development of *In situ* Oil Viscosity Monitoring Technique." I have examined the final copy of this thesis for form and content and recommend that it be accepted in partial fulfillment of the requirements for the degree of Master of Science , with a major in Physics.

Dr. Horace Crater, Major Professor

We have read this thesis
and recommend its acceptance:

Accepted for the Council:

Associate Vice Chancellor and
Dean of the Graduate School

Development of *In situ* Oil Viscosity Monitoring Technique

A Thesis

Presented for the

Master of Science

Degree

The University of Tennessee, Knoxville

Shawn C. Dancik

December, 1998

Acknowledgments

I would like to thank those who have assisted me during the course of this thesis. I thank Mike Smith, Linwood Price, Chip Stepanek, Don Williams and Les Crosswy for their assistance during this work. Also, I extend thanks to those who served on the thesis committee: Dr. Horace Crater, major professor; Dr. J.W.L. Lewis and Dr. Christian Parigger. Thanks also to the Arnold Engineering Development Center (AEDC) and Sverdrup Technology Inc., AEDC Group for providing the laboratories and operation personnel necessary for completion of this thesis.

Abstract

It is essential that lubricating oils not degrade to the point of impacting the quality and performance of industrial machinery. Existing oil quality tests, which are conducted in laboratories, are both time and labor intensive. This has typically led to periodic replacement of oil whether needed or not. In this study, fluorescence spectroscopy has been investigated to determine its suitability for *in situ* monitoring of the viscosity of a Mobil heavy to medium weight lubricating oil. It was necessary to find a portion or characteristic of the fluorescence spectrum that was dependent upon changes in the oil viscosity and independent of contaminants which routinely occur in the oil's application. At constant temperature and using a Xenon arc lamp filtered at 340 nanometers (nm) for the excitation wavelength, two such empirical correspondences were found to occur. First, at 420 nm the signal strength of the fluorescence is found to increase as the viscosity of the oil increases. The second relationship's characteristic is the ratio of signal strengths at two key wavelengths of the fluorescence spectrum, approximately the number of counts at 380 nm divided by the number of counts at 365 nm. It is found that this ratio also increases as the viscosity increases. These monitoring techniques employ a small fiber optic probe that will allow easy adaptation to existing machinery. Additionally, the test can be completed in minutes as opposed to hours for conventional viscosity testing. In this study, the presence of high levels of zinc and copper were seen to affect the fluorescence spectra. Methods of distinguishing changes in the spectra that occur from these contaminants are developed. Results of the accuracy of both methods are reported.

Table of Contents

Chapter Page

I. Introduction....1

II. Theory of Viscosity and Fluorescence....3

A. Viscosity....3

B. Fluorescence....6

III. General Experimental Method....10

A. Oil Samples....10

B. Instrumentation....10

C. Data Collection Method....11

IV. Analysis of Spectra....13

A. Signal Strength Change....16

B. Signal Ratio: Gamma Factor....22

V. Application of Analysis Technique....25

A. Signal Strength Comparison....25

B. Viscosity Determination from Gamma....26

IV. Conclusion and Suggestion for Future Research....33

References....35

Appendices....39

Appendix A. AEDC Fuels Laboratory Results....40

Appendix B. Discussion of Naphthalene.....42

Appendix C. AEDC Precision Measurement Equipment Laboratory Results 43

Appendix D. Analysis for.....45

Vita.....50

List of Figures

Figure		Page
2.1	Model of Liquid	4
2.2	Illustration of Fluorescence	7
3.1	Experimental Apparatus	11
3.2	Illustration of Probe Fibers	12
4.1	Illustration of Sample Spectrum	13
4.2	Repeatability Analysis	16
4.3	Fluorescence of Samples at 90°F	17
4.4	Fluorescence of Samples at 90°F	17
4.5	Fluorescence of Samples at 110°F	18
4.6	Fluorescence of Samples at 110°F	18
4.7	Fluorescence of Samples at 140°F	19
4.8	Fluorescence of Samples at 140°F	19
4.9	Viscosity versus Fluorescence Signal at 420 nm at 90°F	21
4.10	Viscosity versus Fluorescence Signal at 420 nm at 110°F	21
4.11	Viscosity versus Fluorescence Signal at 420 nm at 140°F	22
4.12	Viscosity of Oil versus Gamma at 90°F	23
4.13	Viscosity of Oil versus Gamma at 110°F	24
4.14	Viscosity of Oil versus Gamma at 140°F	24
5.1	Slope of Curve Fits versus Temperature	30
5.2	Y-Intercept of Curve Fits versus Temperature	30

B.1 Structure of Naphthalene.....42

B.2 Electronic Energy Levels of Naphthalene.....42

C.1 CCD Detector Response.....43

C.2 Transmission of Bandpass Filter.....44

C.3 Irradiance of Xenon Arc Lamp.....44

List of Tables

Table		Page
5.1	Results of Signal Strength Comparison to Determine Viscosity	26
5.2	Results of Ratio Method to Determine Viscosity at 90°F and 110°F	28
5.3	Results of Ratio Method to Determine Viscosity at 140°F	28
5.4	Result of Ratio Method to Determine Viscosity at 100°F and 120°F	31

I. Introduction

Viscosity is a fundamental parameter in the characterization of fluids and flow processes. It is also a good indicator of oil quality. Because nearly all mechanical equipment and machinery depend on oil lubricants for proper operation and longevity, the quality of the oils used is an important factor.

Numerous methods exist to measure viscosity. Examples of these traditional methods include capillary flow, falling-ball, and rotating disk. These methods have the following limitations: all are non-conducive to in-line analysis, they involve disrupting the oil flow, and all are time and labor intensive. Typically, oil quality testing is bypassed for periodic oil replacement, an acceptable although not an ideal practice. If oil is replaced too frequently, increased costs of labor and resources are incurred, resulting in increased operational cost. If oil is not replaced soon enough, unnecessary machine wear and degradation result.

Recently, numerous spectroscopic studies have been made with the goal of reducing the time required to complete oil quality testing. The techniques of these studies have included mid-infrared absorption[1], Raman scattering[2,3], refractive index analysis[4], and ultra-violet (uv) fluorescence spectroscopy[5-11]. These studies resulted in measurement methods with reduced testing time. However, the majority of these methods were still limited by their sample dilution requirements (to overcome quenching of the uv fluorescence spectrum) and their necessity for laboratory test conditions. The methods reported by Goetsch [4] and Friesen [10] have been implemented into in-line analyses in oil production processes, but they were still hampered by long response times

for detection of changes in viscosity [4] or required extensive effort to incorporate into the existing machinery [10]. A more practical test method would require no dilution of the oil and would allow *in situ* testing. Of the possible methods, measurement of uv fluorescence offers good potential for *in situ* monitoring, because it is relatively simple mechanically, potentially portable, and easily implemented via a probe that will not affect the oil flow [12]. Additionally, uv fluorescence has been examined and demonstrated to be effective in other applications such as locating crude oil spills on ocean surfaces from instruments mounted on aircraft [13,14,15]. These studies demonstrated that the fluorescence spectrum of an oil sample can successfully be used to determine characteristics of that sample.

An oil viscosity-monitoring instrument used on industrial machinery, as opposed to use in an oil refinery, must be able to give accurate readings when the oil becomes contaminated. If such a reading is not possible, the system must be able to identify the presence of the contaminants and indicate that the viscosity reading may not be accurate. Work on such a uv fluorescence method and system is discussed herein.

II. Theory of viscosity and fluorescence

A. Viscosity

In this study, the fluorescence properties of the oil samples are empirically related to the oil's kinematic viscosity. Determination of kinematic viscosity is a measurement that is typically performed and is one of the measurements conducted by the AEDC fuels laboratory to check oil quality. To give a concise definition of kinematic viscosity, it is first necessary to define absolute viscosity and discuss the concept of shear flow. Absolute viscosity is defined as a fluid's resistance to shear flow. Whenever written alone, the term viscosity typically refers to the absolute viscosity. Shear flow is fluid motion for which there exists a velocity gradient perpendicular to the flow velocity. The difference in flow velocity results in the fluid slipping over itself. With these terms defined, kinematic viscosity is itself defined as the absolute viscosity of the fluid divided by the density of the fluid [16]. The preferred units of measure here are in the cgs system; units for the absolute viscosity is the poise (dyne • sec / cm^2) and for the kinematic viscosity is the stoke (cm^2/sec).

The theory of the viscosity of liquids is in general complicated. The process is thought to involve many molecules and be highly complex [17]. A simplified model is, however, available from hole theory [17], a development which appears to be attributed primarily to Eyring [18,19]. A liquid can be modeled as in Figure 2.1, where δ is the distance between planes of molecules, a is the distance between neighboring sites and F is the external force per unit area tending to displace one layer of molecules with respect to another [18]. In this model, the total number of molecules is less than the total number

of sites. The following derivation follows that of Eyring and considers the motion of molecules into a nearby vacant sites (or holes). These molecules must squeeze through the smaller region, or bottleneck, formed by its nearest neighbors.

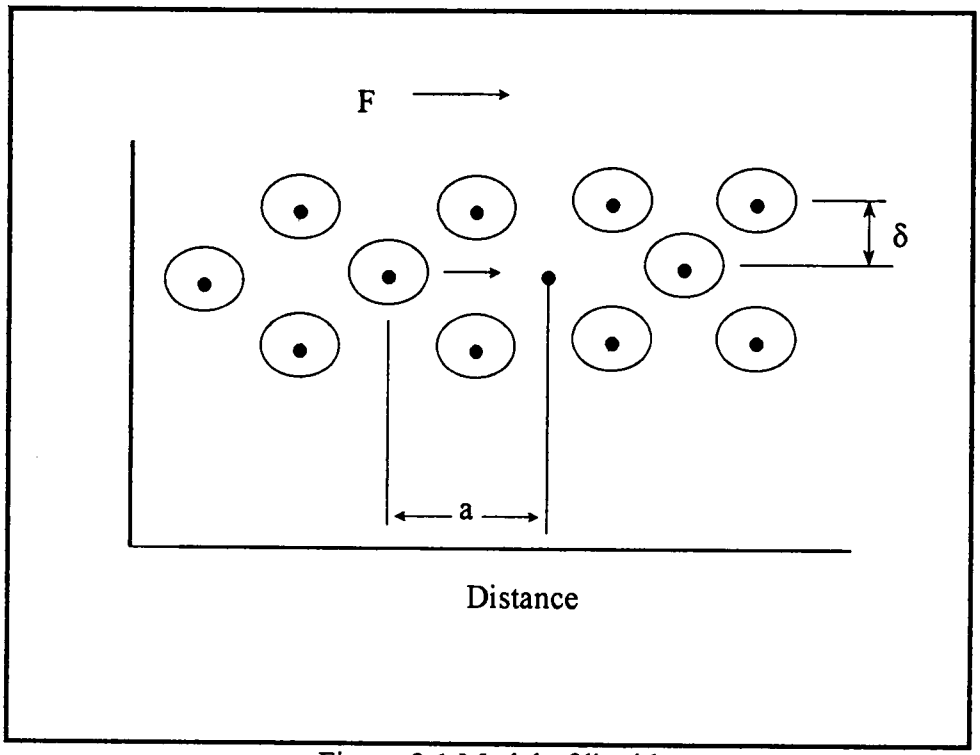


Figure 2.1 Model of liquid

Defining the forward process as the movement of a molecule into a hole in the direction of F and the reverse process as the movement of a molecule into a hole in the opposite direction of F, the net velocity of flow of the fluid with respect to the sites is,

$$v_o = a(k_f' - k_r') \qquad \text{Equation 2.1}$$

where k_f' and k_r' are the frequencies of the forward and reverse processes. They can be written as,

$$k_f' = k_o' \exp[{}^{aF}/_{2\,n\delta kT'}] \qquad \text{Equation 2.2}$$

$$k_r' = k_o' \exp[-{}^{aF}/_{2\,n\delta kT'}] \qquad \text{Equation 2.4}$$

where k_o' is the value of k_f' and k_r' in the absence of F, n is the number of molecules per unit volume, k is the Boltzman number and T' is the temperature in Kelvin. The net flow v_o can now be written as,

$$v_0 = 2a\, k_o' \mathrm{Sinh}(aF/2\, n\delta kT') \qquad \text{Equation 2.5.}$$

By substituting this result into the definition of the coefficient of viscosity, the following equation is obtained,

$$\eta' = \{ F/(v_0/\delta) \} = \{ F\delta/ 2a\, k_o' \mathrm{Sinh}(aF/2\, n\delta kT') \} \qquad \text{Equation 2.6.}$$

An order of magnitude calculation shows that the argument of the sinh function is 2.97×10^{-8} (newtons^{-1}•meters^2) times the magnitude of F (newtons•meter^{-2}). Taking the first term of the Taylor expansion of sinh results in Equation 2.7.

$$\eta' = (\delta/a)^2(nkT'/k_o') \qquad \text{Equation 2.7.}$$

Applying Eyring's rate equation,

$$k_o' = (kT'/h)e^{-\Delta E / 2.45RT'} \qquad \text{Equation 2.8}$$

where ΔE is the energy of vaporization, R is the gas constant 8.314 J•mol^{-1}K^{-1} and h is Plank's constant. Equation 2.8 can thus be written as,

$$\eta' = (\delta/a)^2 nhe^{+\Delta E / 2.45RT'} \qquad \text{Equation 2.9.}$$

This equation shows that for liquids, the viscosity decreases with increasing temperature. This is a striking contrast between the relationship of viscosity and temperature for gases [18]. In gases the viscosity raises as the square root of the temperature. The energy of

vaporization appears in these equations because the bonds between neighboring molecules must be broken to make a hole [18]. These are the same bonds that are broken during the vaporization process [18].

B. Fluorescence

Fluorescence, which includes light emission resulting from electron transitions between electronic states of molecules, occurs when light of a particular wavelength is absorbed by a compound and then re-emitted usually at a longer wavelength [20]. This discussion does not include the possibility that collisions can add additional energy to electrons. That circumstance allows for emission of light at shorter wavelengths. This process was not experimentally observed in this study and will not be further discussed in this overview. The explanation of fluorescence is based on Bohr's postulate that energy levels available to electrons are quantized. An electron in a lower or ground state can only be excited to a higher level if the excitation energy incident upon that electron matches the energy difference between the electron's present level and a higher level. Once in a higher energy state, the electron attempts to release its extra energy and return to a lower state. When a broad excitation source is used at with an arc lamp, multiple such transitions take place causing a broadened fluorescence spectrum.

This process is shown in Figure 2.2 for an arbitrary system. The bold lines (S_n) denote the electronic energy levels while the thin lines denote the vibrational energy levels. The arrows illustrate some of the possible transitions. The energy difference between neighboring rotational energy levels is typically only 0.01 - 0.001 eV [21]. In

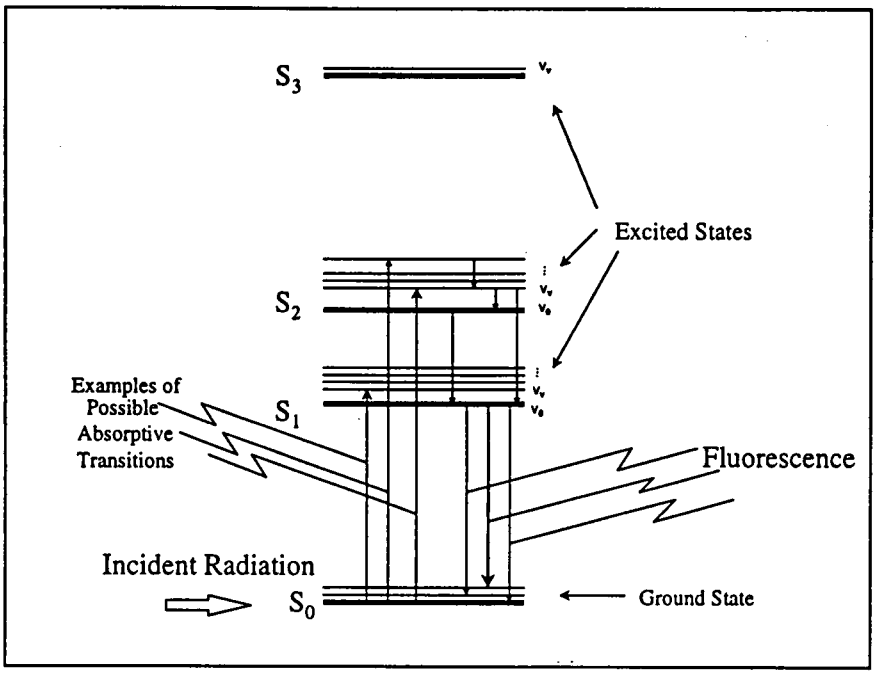


Figure 2.2 Illustration of Fluorescence

aromatic molecules (defined below) in the liquid state these rotational levels are collisionaly broaden to the extent that they become a continuum. These levels are therefore not included in the figure. The order-of-magnitude of the energy differences between neighboring vibrational and electronic energy levels are typically 0.1eV and several eV respectively. Fluorescence results from a system being excited into an upper state by absorption of radiation and then decaying back to a lower state in a time typically less than 10^{-5} seconds [22]. More specifically, the absorbed radiation promotes the system into one of the higher vibrational levels of an excited electronic state S_n (n =1,2,3,...). The system then drops down through the vibrational levels (vibrational relaxation) to the $S_1(v = 0)$ level and eventually decays back through the series of vibrationally excited levels of the ground electronic state $S_0(v = 0, 1, 2,...)$ [22]. The

transitions between electronic states (S_1 - S_0) result in the fluorescence while the vibrational relaxation results in broadening of the fluorescence. Further discussion of the fluorescence of the particular molecule of interest in this work is given below.

Fluorescence in the uv region has been found to occur in numerous types of crude oils [8,13]. All crude oils are composed of four basic components; saturated hydrocarbons, aromatic hydrocarbons, resins and asphaltenes [23]. A hydrocarbon is a compound that contains only hydrogen and carbon. Aromatic hydrocarbons are distinguished by their structures. To be aromatic, a compound must be both cyclic and planar [24]. It is the aromatic hydrocarbon content in the oil that, upon uv irradiation, is responsible for the fluorescence spectra [24].

In order to understand the measured spectrum observed in this study, an attempt was made to determine what molecules are being excited and are fluorescing. To determine which organic compounds were present, the AEDC chemistry lab analyzed a sample of oil. The results from the chemistry lab showed that none of the compounds capable of being detected by their instruments were present in detectable amounts. The complete list of compounds tested is given in Appendix A.

It is felt, however, that naphthalene ($C_{10}H_8$) may still exist in the oil. The manufacturer alluded that naphthalene could be present [27]. The structure and energy level diagrams of naphthalene are shown in Appendix B for reference. Due to the chemistry lab results, further discussion of the origin of the appearance of the spectral signature (a double peak) based on naphthalene presence seems improbable. However, there are at least three references that associate a double peak structure with the presence

of naphthalene [21,28,29]. In these publications, naphthalene was used as a dopant; therefore it is not unreasonable to assume that naphthalene is present here at a concentration that (although undetectable by the use of standard chemistry laboratory procedures) is sufficient for a viscosity measurement.

It is also possible to develop a qualitative understanding of the relationship between viscosity and fluorescence. In Equation 2.3, the viscosity was shown to be dependent on the energy between neighboring molecules. As the viscosity is decreased, the bonds become weaker allowing greater motion of molecules relative to one another. This leads to an increase in the number of collisions. When the oil is irradiated with light, these molecules will release the additional energy they absorb. They can do so either by radiation (fluorescence) or a non-radiative process (i.e. collisions). As the number of collisions increases (due to lower viscosity), the fluorescence signal strength is decreased, or collisionally quenched [5]. Therefore, as viscosity is increased the fluorescence signal will also be increased.

III. General experimental method

A. Oil samples

The oil samples used in this experiment were taken from bearings of the twelve compressors of the sixteen foot propulsion wind tunnel at AEDC. The oil used in these bearings is a Mobil heavy to medium weight lubricating oil. The oils in different bearings experience different usage times and different wear conditions, so these samples had different viscosities and contained different wear metal contaminants. One sample of new oil was also tested.

B. Instrumentation

A Santa Barbara Instrument Group astronomical ST-6 CCD camera with adaptive spectroscopic software was used in conjunction with an Oriel 1/8 meter crossed Czerny-Turner spectrograph to collect the spectra. A 75-watt Xenon arc lamp, with an appropriate housing, power supply and focusing lens assembly, was used as the excitation source. A ten nanometer bandpass filter selected 340 nm as the excitation wavelength. To allow for *in situ* applications in the future, the apparatus used individual Polymicro Technologies Incorporated uv enhanced silica fibers, with 400 micron diameters, for transportation of the excitation and emission light. These fibers have an attenuation of 358 decibels per kilometer at 250 nm. The fibers were coupled to the lamp and spectrograph with fused silica lenses. To determine the quality and reliability of these instruments, the bandpass filter, the CCD camera and the Xenon arc lamp were tested and calibrated by the Precision Measurement Equipment Laboratory (PMEL) at AEDC. The results are graphically displayed in Appendix C. The apparatus is shown in Figure 3.1.

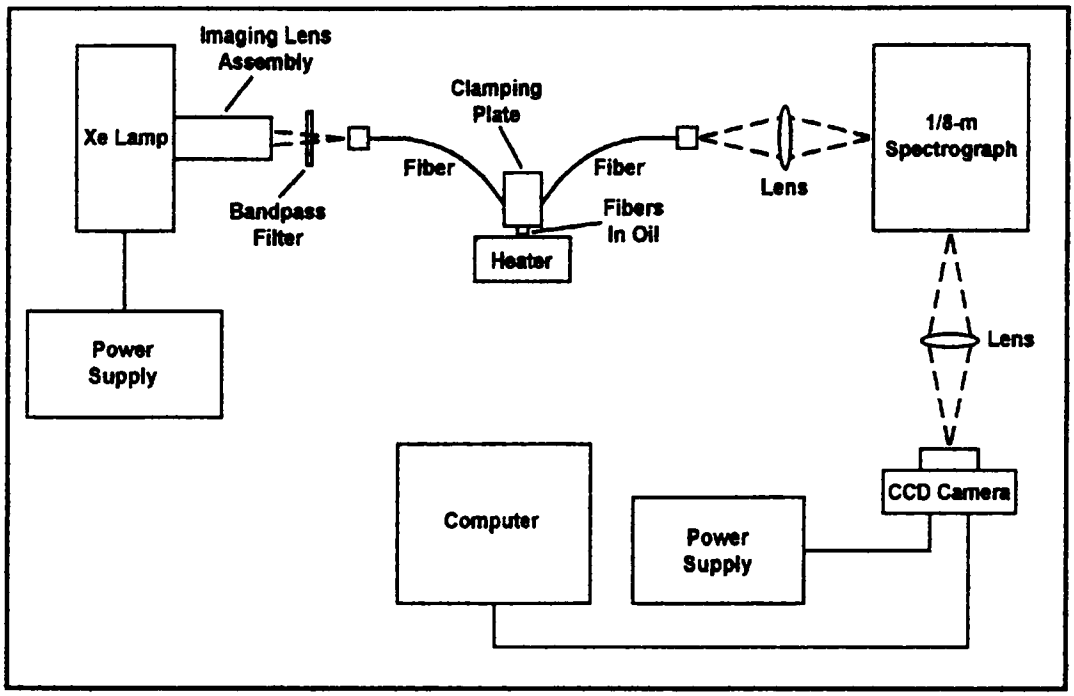


Figure 3.1 Experimental apparatus

C. Data collection method

The oil samples were heated to a temperature in the range of 80°F to 140°F (it is preferred to report Fahrenheit units for the presentation of the temperature dependent viscosity results to be consistent with AEDC chemistry laboratory methology). This range covers the nominal variations in temperature experienced in the bearings. At intervals of 10°F, a five-second exposure was taken of the fluorescence. During data acquisition, the camera was internally cooled to reduce noise, and the oil samples were continuously stirred. The stirring was necessary to eliminate the loss of fluorescence

signal due to the photo-degradation of the fluorescing molecules. This loss of signal could have been misinterpreted as a resultant of oil properties.

To ensure that no cross contamination of the oils occurred and that changes in the spectra could be attributed solely to changes in the oil, the fibers were epoxyed in position and thoroughly cleaned between each trial. The cleanliness of the fibers was verified by taking an exposure with the fibers in air. When no fluorescence signal persisted, the oil was determined to be completely removed. The two fibers (excitation and emission) were separated by an angle of approximately 80°, see Figure 3.2. This angle was chosen because it allowed easy insertion of the fibers into a sample and effective collection of the fluorescence signal. The ends of the fibers were immersed in the oil during data collection.

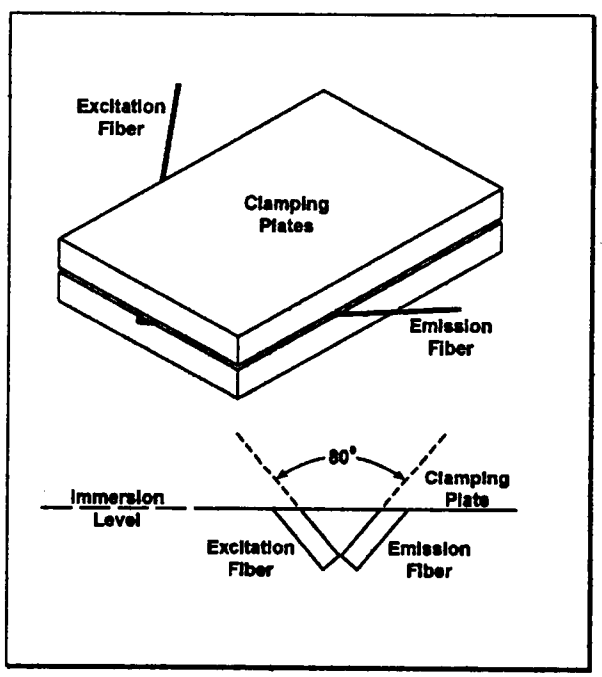


Figure 3.2 Illustration of probe fibers

IV. Analysis of spectra

After the spectra were collected, they were examined for a correlation of changes in the spectra with changes in viscosity. Two analysis methods were pursued. The first was a simple comparison of emission signal strength at a particular wavelength, 420 nm, to viscosity. This method was similar to the work done by Keller and Saba [7]. The second method analyzed the ratio of the signal strength at the minimum between the two

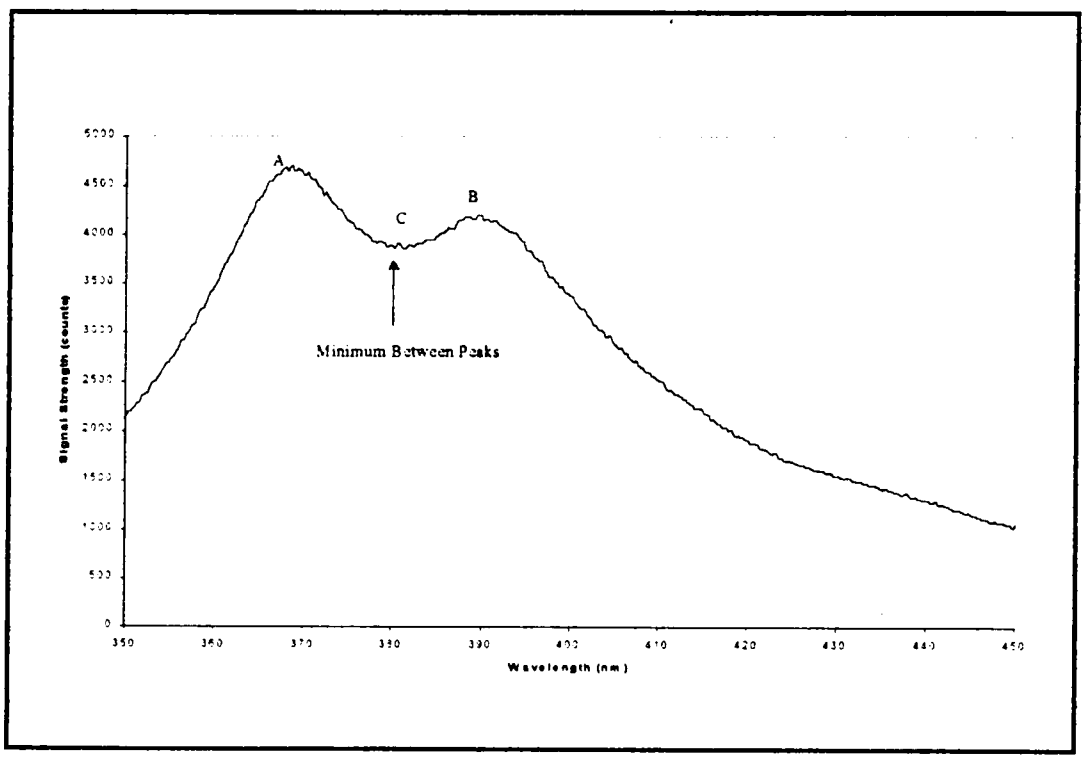


Figure 4.1 Illustration of sample spectrum

peaks (labeled C; Figure 4.1) in the spectrum to the maximum signal strength at the first peak (labeled A; Figure 4.1). It is to be noted that the shape of this spectrum is similar to that reported by Berlman for naphthalene [21]. If this oil does contain naphthalene, the peaks labeled A and B can attributed to a monomer (M) and an exciplex (E) signal respectively [28]. An exciplex is a complex that only exists in the excited state. It is

formed during the reaction of a ground state organic molecule with an excited state organic molecule [28]. A double peaked fluorescence spectrum resulting from an excimer and monomer is described by the following reaction if excited by a laser source:

$$M + \hbar\omega_o \rightarrow M^* \qquad \text{Equation 4.1}$$

$$M^* + G \leftrightarrow E^* \qquad \text{Equation 4.2}$$

$$M^* \rightarrow M + \hbar\omega_1 \qquad \text{Equation 4.3}$$

$$E^* \rightarrow E + \hbar\omega_2 \qquad \text{Equation 4.4}$$

where M^* is the excited state organic molecule, G is the ground state partner and E^* is the exciplex [28]. If a broad band source is used for the excitation, the emission signals are broadened to include multiple wavelengths each. A double peak emission spectrum would be depicted by two sets of possible fluorescence transitions (see Figure 2.2, Section II.B). The fluorescence from the E^* transitions is red shifted due to energy required to form the chemical bond. At temperatures which included the range investigated here, Murray and Melton has stated that the formation of the exciplex increases with increasing temperature due to the kinetic effect of decreasing viscosity [28]. The exciplex peak has also been seen to have a strong temperature dependence at temperatures greater than 212°F [29].

The ratio of the signal strengths at locations C and A (abbreviated gamma from this point forward) was then compared to kinematic viscosity. Additionally, for both analysis techniques, the amount of wear metal in each sample was taken into consideration by looking for contaminant levels that were higher than the average. This data was supplied by the AEDC fuels laboratory through atomic emission analysis.

Before a discussion of the application of these methods to determine the viscosity is undertaken, the repeatability of the data collection method is presented. Twelve spectra were collected for a single sample at a constant temperature. Four of the twelve spectra are shown in Figure 4.2. The data was taken in four sets (one from each set is shown in Figure 4.2). Each set consisted of four exposures immediately following each other. After the first set was collected, the fibers were removed from the oil and cleaned. The system was then completely shut down. After all of the instruments were allowed to cool down, the system was then powered on and the second set of four spectra were collected. Then, without removing the fibers, the temperature of the oil was allowed to climb and then return back to the original temperature where four more spectra were collected for the third set. This last step was repeated a second time to obtain the fourth and final set. The average number of counts at 420 nm for the twelve spectra was 1427 counts. The maximum and minimum values were 1507 and 1367 counts respectively. The precision was ±2.9% to one standard deviation for the fluorescence counts values. The average value of gamma was 0.6791. The maximum and minimum values were 0.6835 and 0.6728 respectively. The precision was ±0.57% to one standard deviation for the values of gamma.

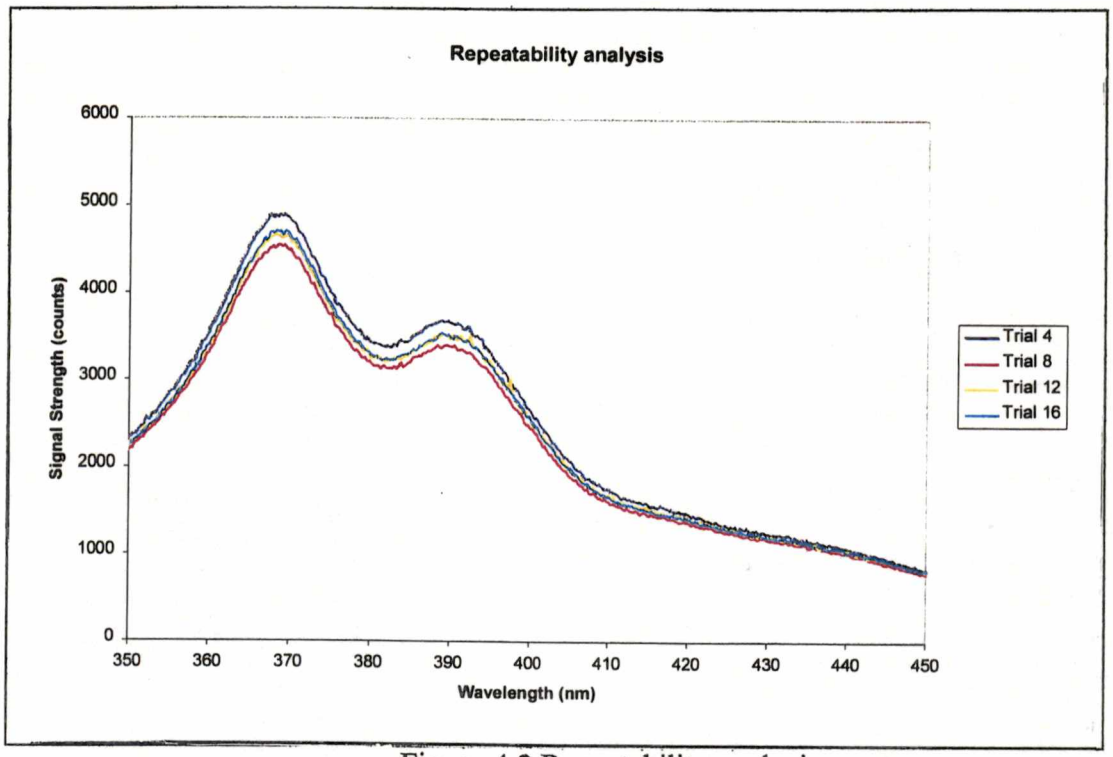


Figure 4.2 Repeatability analysis

A. Signal strength change

Figures 4.3 - 4.8 show the fluorescence spectra of the thirteen oil samples at constant temperatures of 90°, 110°and 140°F. For clarity, each graph displays only half of the spectra collected (one from each oil sample) at the indicated temperature. The three temperatures displayed were the temperatures at which the viscosity was measured by the AEDC fuels laboratory and are representative of the data collected across the temperature range investigated.

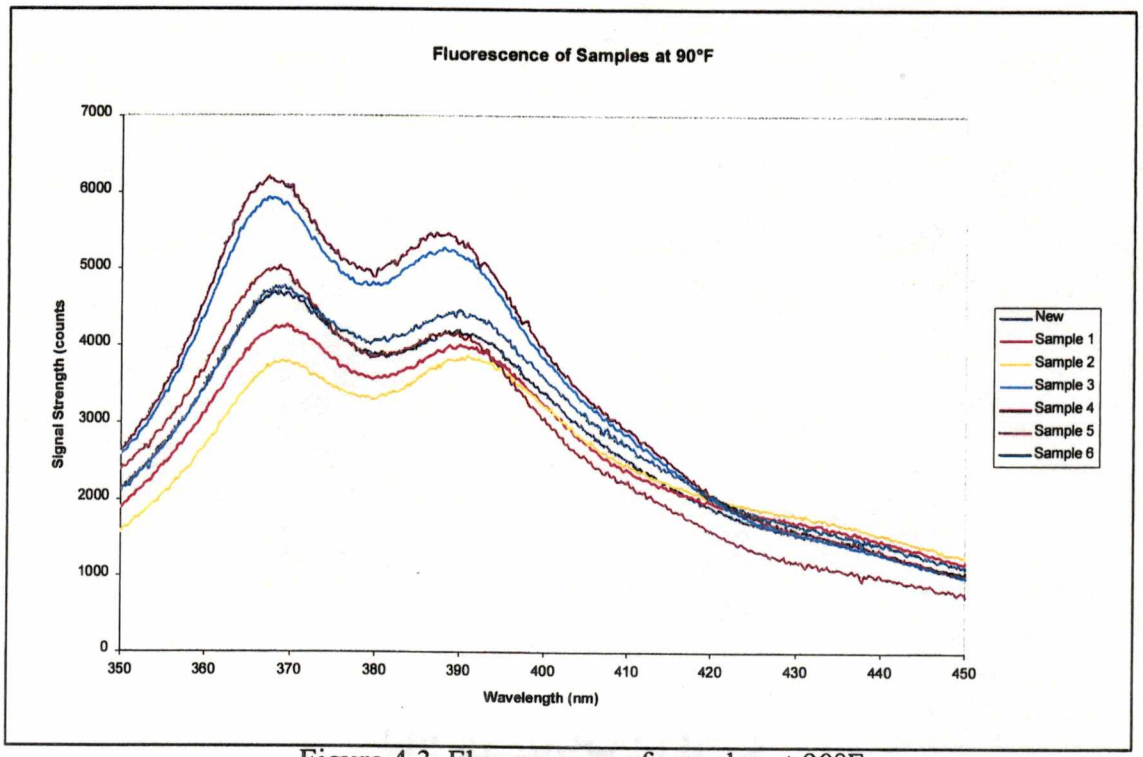


Figure 4.3 Fluorescence of samples at 90°F

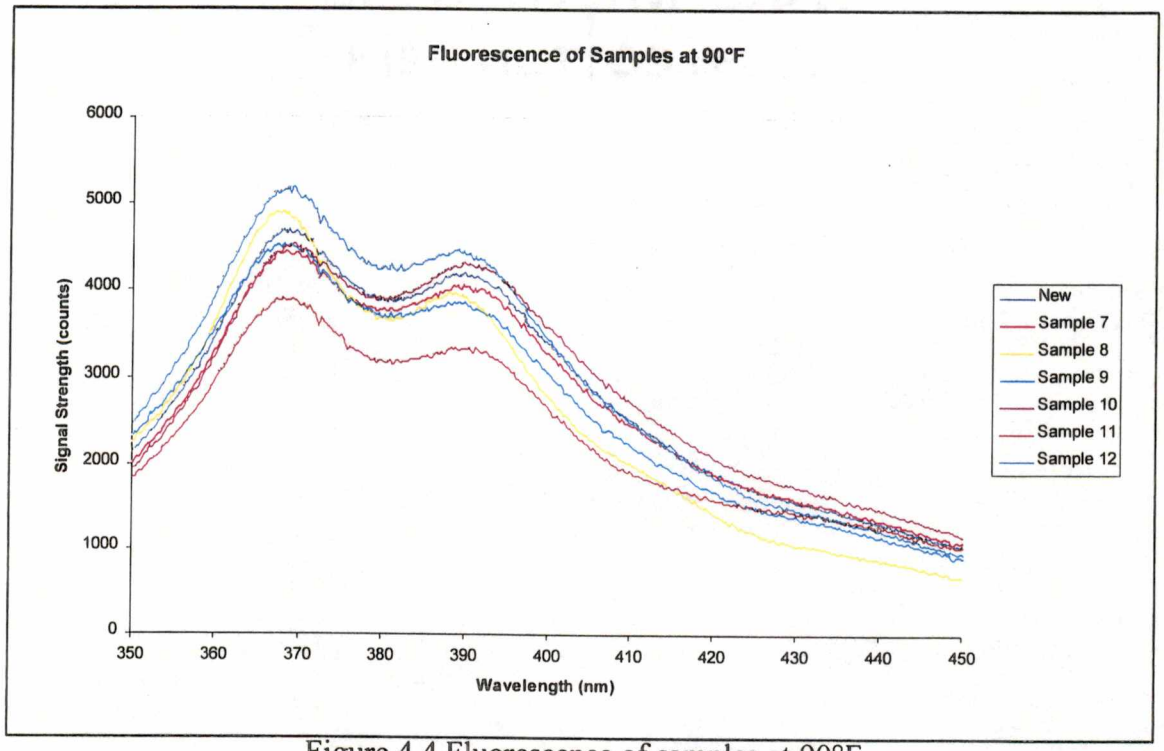


Figure 4.4 Fluorescence of samples at 90°F

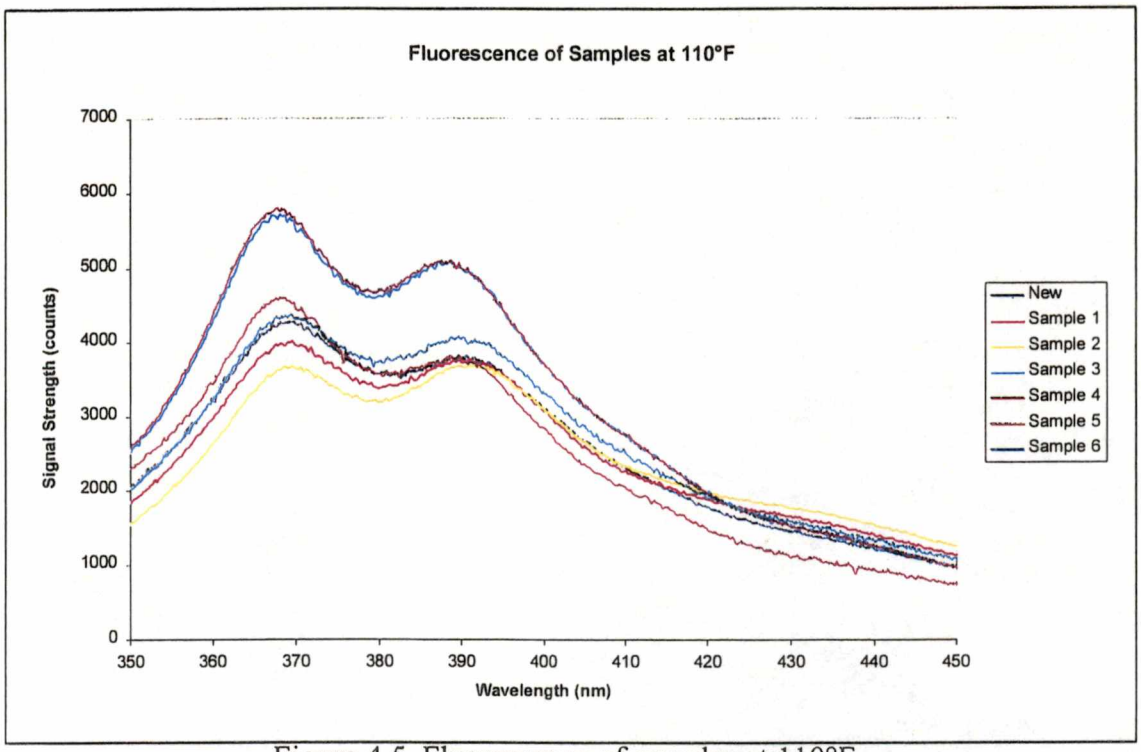


Figure 4.5 Fluorescence of samples at 110°F

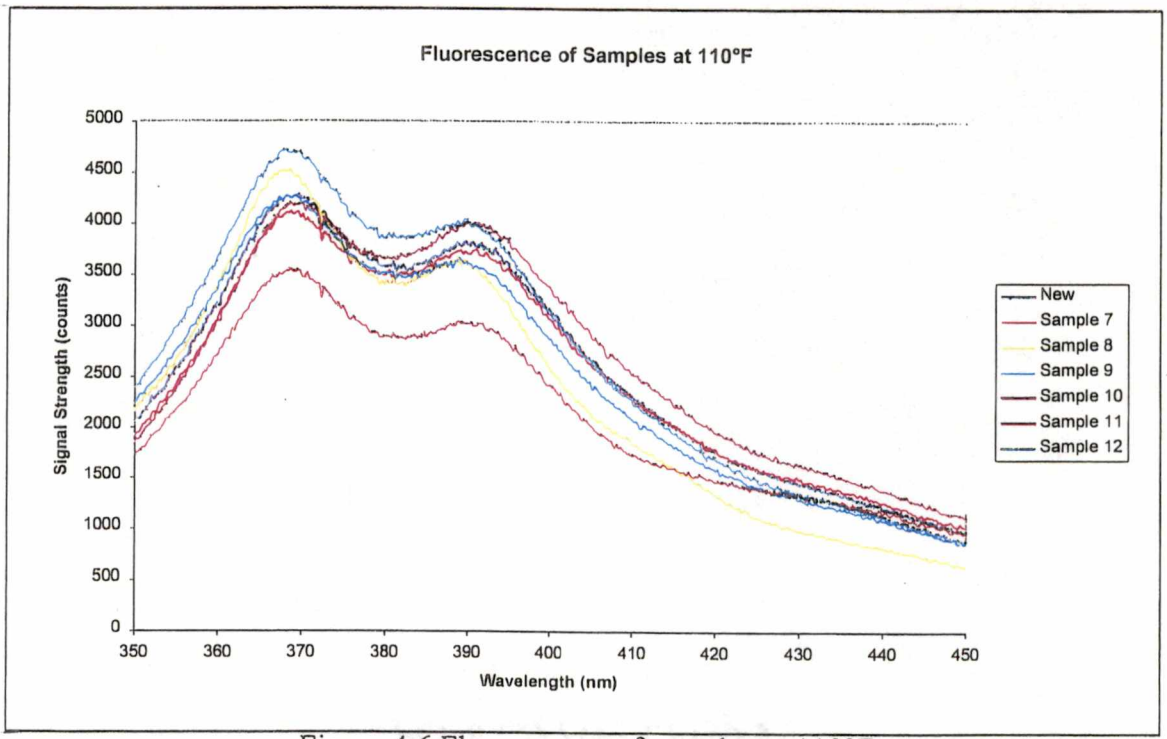


Figure 4.6 Fluorescence of samples at 110°F

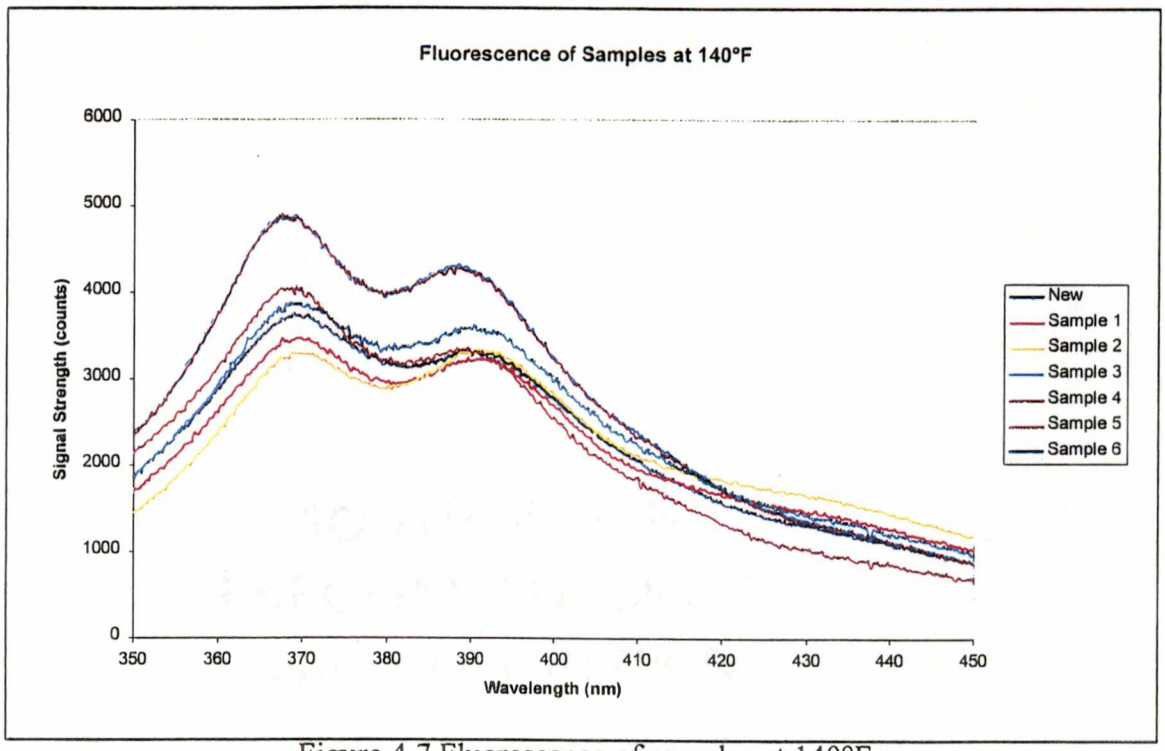


Figure 4.7 Fluorescence of samples at 140°F

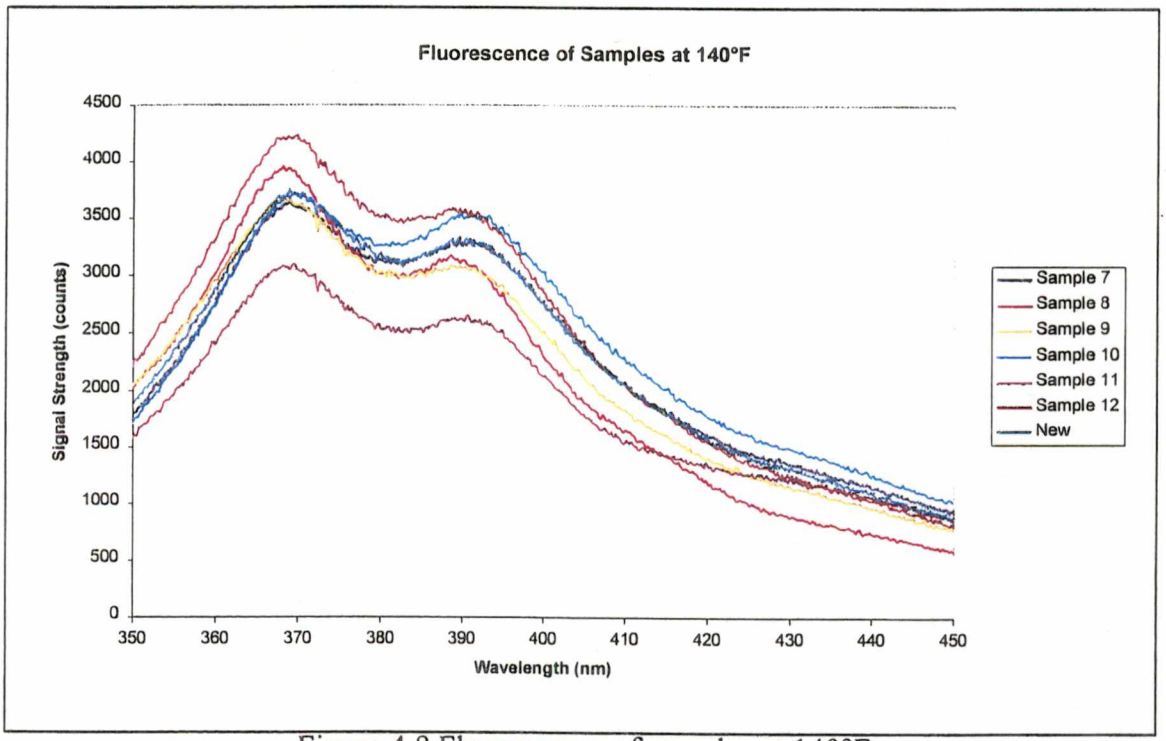


Figure 4.8 Fluorescence of samples at 140°F

The data from the wear metal analysis and the viscosity measurements were compared to the fluorescence at 420 nm of each sample, one of which was the new sample. That wavelength was chosen because the signal strength at 420 nm appeared to be relatively resistant to change when contaminant levels were high. Additionally, the data was analyzed to determine changes in the spectra that corresponded solely to the presence of high levels of wear metals. If a correlation between viscosity and signal strength is not possible due to the presence of wear metals, a mechanism needs to be developed which will recognize the presence of the contaminant. A change resulting from high contaminant levels should not be mistaken for a change in viscosity.

Figures 4.9, 4.10 and 4.11 show the variation of fluorescence signal strength at 420 nm versus viscosity for the oil samples. Four of the thirteen samples were arbitrarily withheld to be used later to predict their viscosities with this method. The points labeled High Copper Content in these figures contained significantly higher levels of copper than the average of the other six samples. One additional data point is not displayed on the graphs. It contained high levels of Zinc and did not fall with in the range displayed on the graphs. Because of these excesses in contaminant content and unique fluorescence data, they were not included in the calculation of the curve fit.

It was also noted that the spectra of sample 3 and sample 4, in Figures 4.3, 4.5 and 4.7 both have an unusual property. Large portions of the spectra from these two samples have signal strengths that are larger than the signal strength of the new oil spectrum even though the new sample had a higher viscosity. These samples contained high zinc levels. Without considering the presence of the contaminants, this fact is in apparent anomaly to

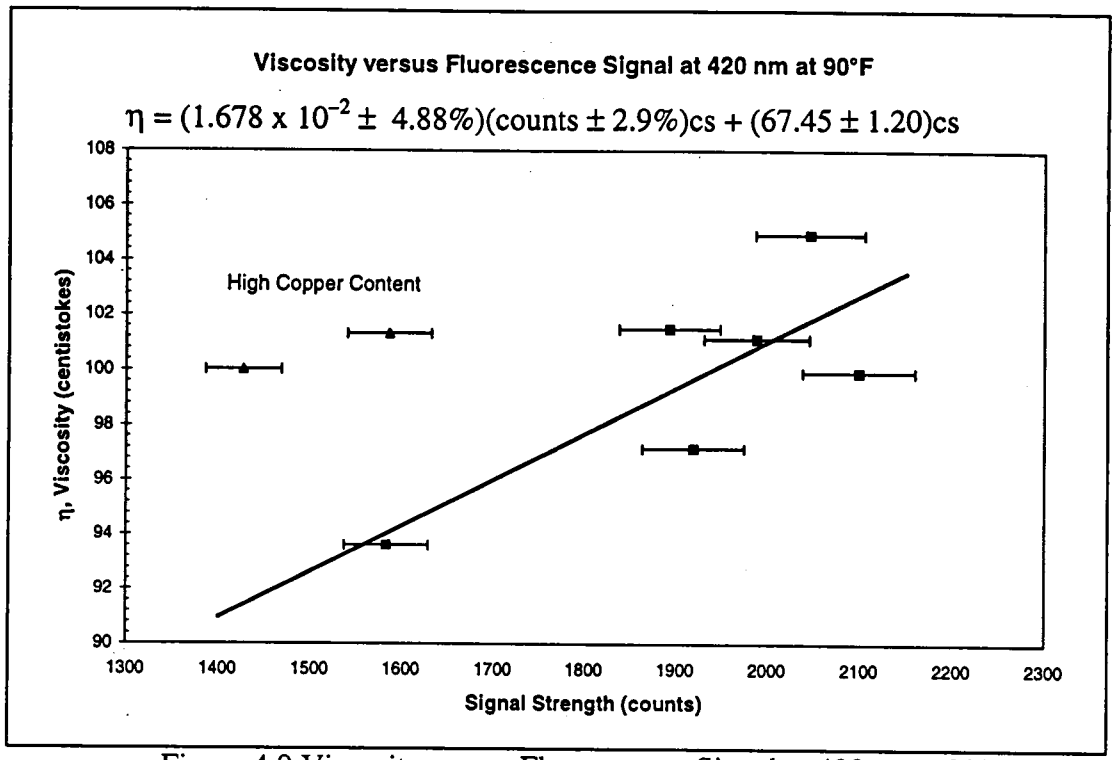


Figure 4.9 Viscosity versus Fluorescence Signal at 420nm at 90°F

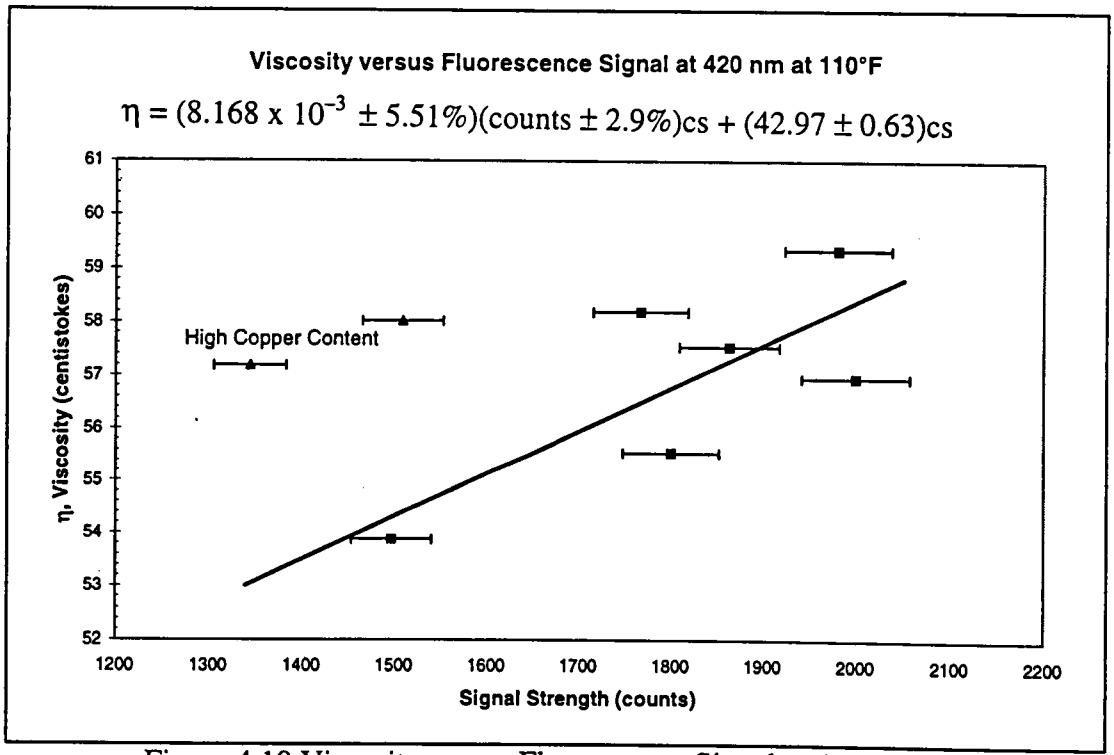


Figure 4.10 Viscosity versus Fluorescence Signal at 420nm at 110°F

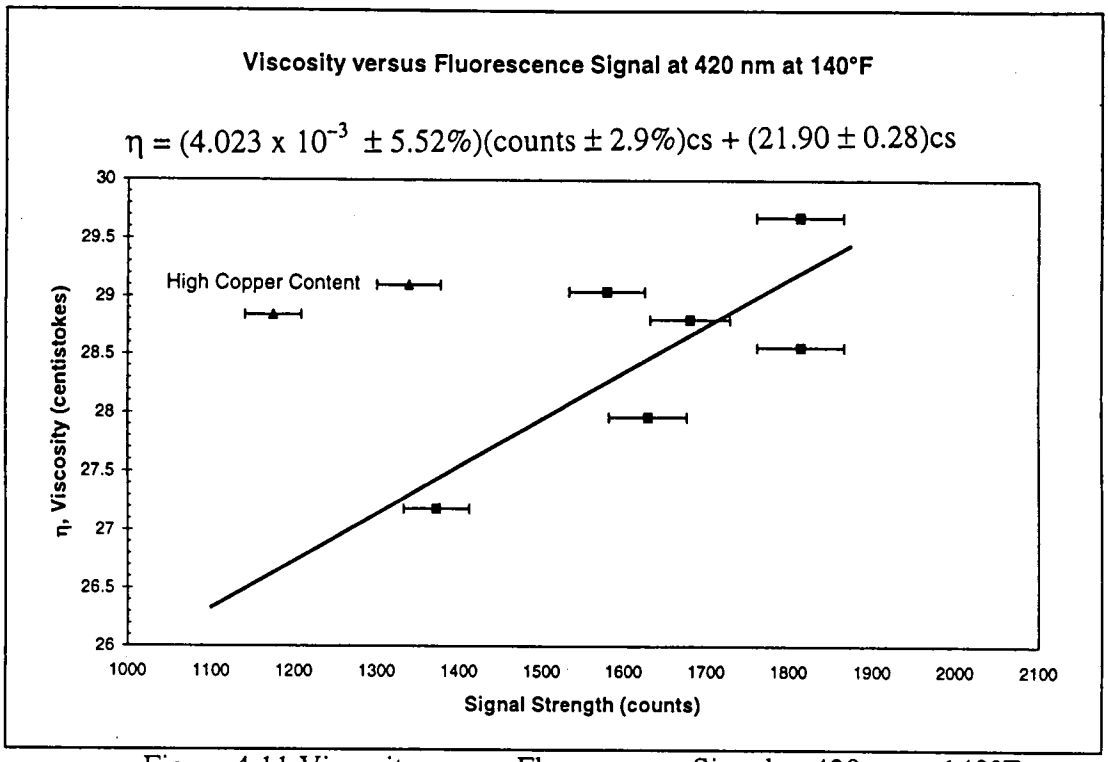


Figure 4.11 Viscosity versus Fluorescence Signal at 420nm at 140°F

previous studies that found a decrease in fluorescence signal strength with a decrease in viscosity [7]. Except for these two examples, the data agrees with the work of Keller and Saba [7]. The main difference between this work and that study is the inclusion of samples that contain wear metal particles. The results of using these relationships (the curve fits in Figures 4.9 - 4.11) to predict the viscosity of oil samples are given below.

B. Signal Ratio: Gamma Factor

As an alternative to comparing variations in signal strength at a particular wavelength, a second analysis technique was investigated. Here the ratio of the relative minimum between the two main fluorescence peaks versus the maximum signal strength

of the second peak (see Figure 4.1) was plotted against viscosity. Figures 4.12, 4.13 and 4.14 show the graphs of viscosity versus gamma at 90°F, 110°F and 140°F. For this comparison, two sets of oil samples taken from the bearings were used. The first set was used to produce Figures 4.12- 4.14. The second set was taken from the bearings five months before the first set and used to test the accuracy of the curve fits. In Figures 4.12-4.14, the point labeled High Copper Content had 428% more copper than the average of the other samples. An additional data point fell outside the range of these figures which contained a high level of zinc. Results of the ability of this method to determine viscosity are also given in the next section.

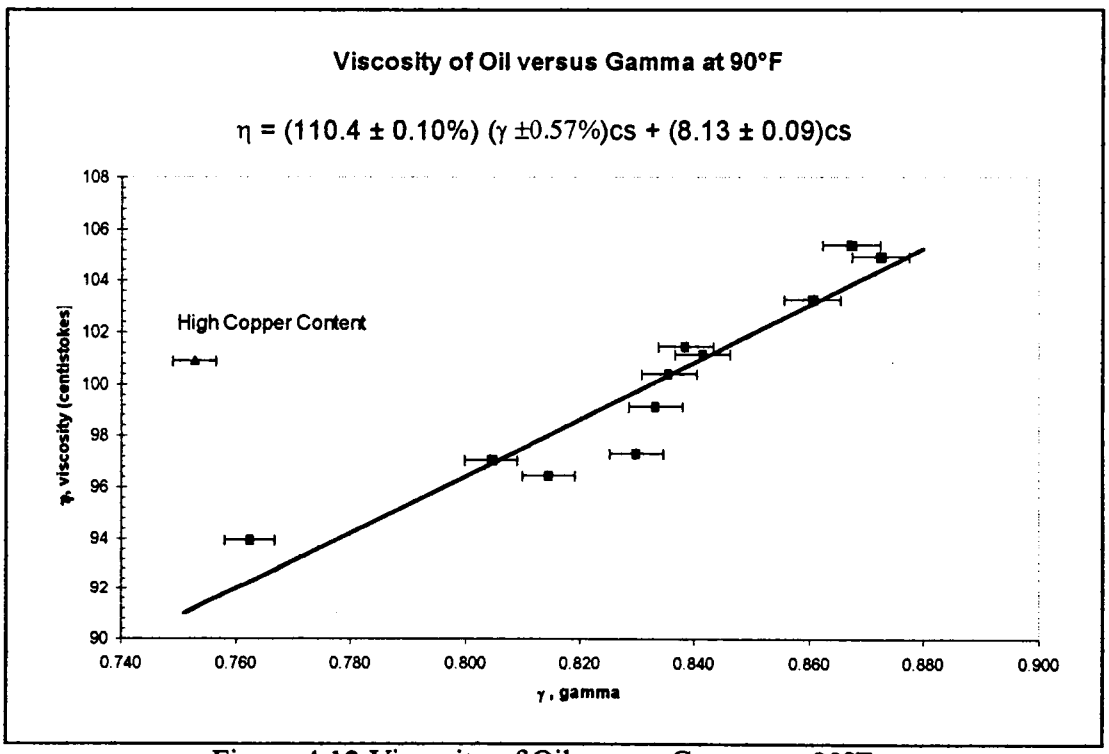


Figure 4.12 Viscosity of Oil versus Gamma at 90°F

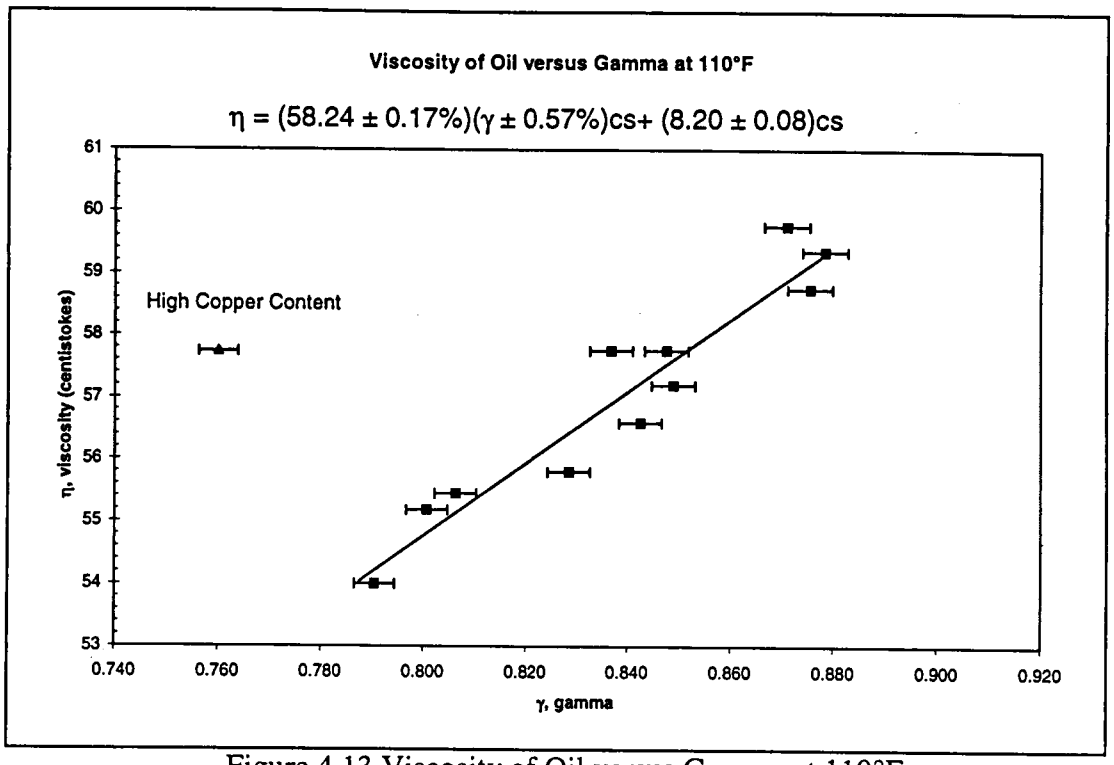


Figure 4.13 Viscosity of Oil versus Gamma at 110°F

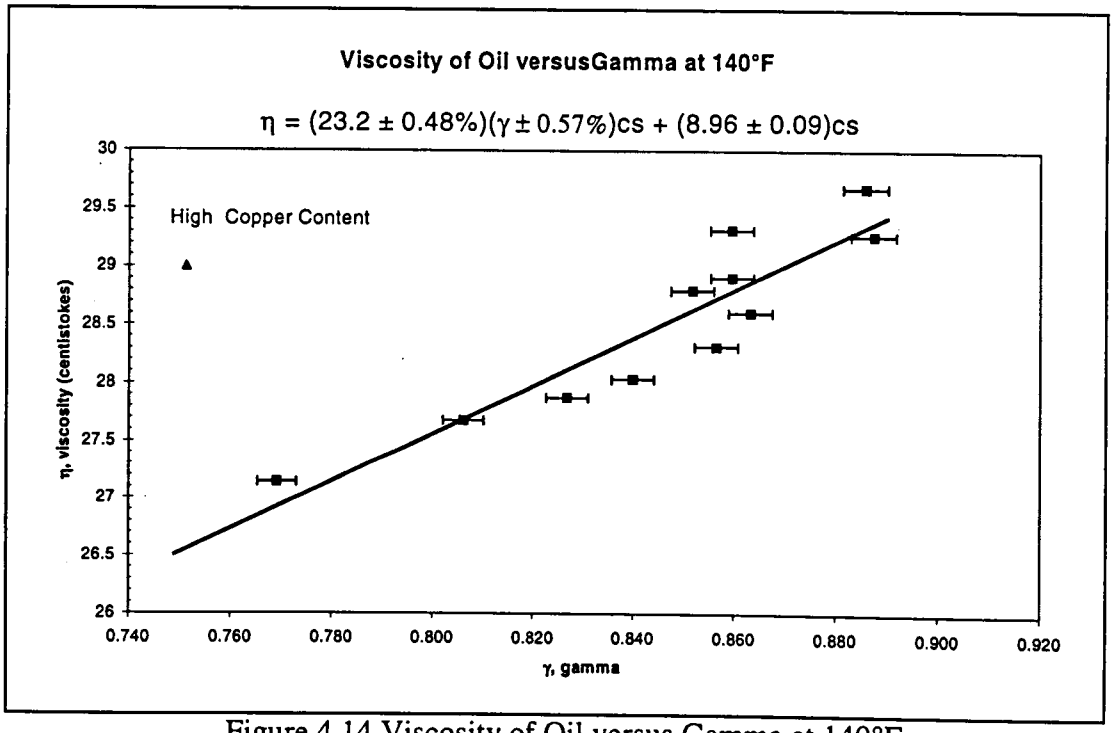


Figure 4.14 Viscosity of Oil versus Gamma at 140°F

V. Application of analysis techniques

A. Signal strength comparison

To utilize these findings in a rapid manner, a program was written in Fortran to accept the spectrum data from the CCD camera. It was necessary to save the data file from the camera in ASCII format. The program, analysis.for, is given in Appendix D. It requires as input the filename under which the spectrum is saved and the temperature of the oil when the spectrum was collected. The program then reads the fluorescence signal strength at 420 nm and computes the viscosity of the oil by using the viscosity vs. signal strength curve fits for the appropriate temperature (see Figures 4.9-4.11, Section IV.A). Calculation of the viscosity is done in subroutine Viscosity. The program also compares the peak signal strength of the spectrum to the peak signal strength of the new oil spectrum by means of subroutine zincwarn. If the peak strength is greater than the new oil peak by at least fifty counts, the program returns a warning that the zinc level may be high; hence alerting the user that the viscosity reading may be inaccurate. This was done to avoid misidentifying spectral changes, such as in samples three and four of Figures 4.3, 4.5, and 4.7, as resulting from changes in viscosity; since the difference appears to be the result of the high levels of contaminants. Table 5.1 shows the results of using these curve fits to predict the viscosities of the final four samples withheld from the full sample set, as discussed earlier. The columns titled viscosity contain the viscosity values determined by the AEDC chemistry laboratory. The columns titled measured viscosity contain the viscosity values determined by the program analysis.for.

Table 5. 1 Results of the signal strength comparison to determine viscosity

Sample	Viscosity (cs) 90°F	Measured Viscosity (cs) 90°F	Viscosity (cs) 110°F	Measured Viscosity (cs) 110°F	Viscosity (cs) 140°F	Measured Viscosity (cs) 140°F
3	75.35	101.40 ± 3.12	44.34	58.09 ± 1.63	23.10	28.92 ± 0.72
6	101.32	102.39 ± 3.18	56.39	57.68 ± 1.60	28.32	29.08 ± 0.73
9	95.60	95.74 ± 2.80	54.73	55.18 ± 1.44	27.55	27.58 ± 0.63
12	96.76	99.08 ± 2.99	55.35	56.11 ± 1.50	27.92	28.18 ± 0.67

Excluding sample three, which was seen to have a high level of zinc, the mean of the absolute value of the accuracies was 1.3%. This value is within the precision of the data. The subroutine zincwarn was successful in alerting the presence of the high zinc level in sample three.

This method does have certain limitations. It is sensitive to changes in the alignment of the equipment and variations in the intensity of the excitation light. Differences in either of these two aspects could be mistaken for changes in viscosity. A normalization procedure would be needed before implementation of this method. Additionally, recognition of spectral changes due to high levels of wear metals, other than zinc, is difficult.

B. Viscosity Determination from Gamma

The program, analysis.for, was again used to facilitate the calculation of the viscosities from gamma. The curve fits of Figures 4.12-4.14 were programmed in subroutine Vis_Gamma. Tables 5.2 and 5.3 display the results of using these curves to predict the viscosity values.

Again, in the absence of high contaminant levels, the predicted values were close to the actual values. Samples five and eight contained high levels of zinc and copper, respectively. Excluding these samples the percent errors ranged from -3.7% to +7.6%.

It was further noted that when the contaminant levels are high, gamma was approximately 0.7600 or less. This observation can be easily utilized to distinguish a change in the spectrum that is due to the contaminant levels, not due to a variation of the viscosity.

Using gamma to determine viscosity is less sensitive to alignment changes than the previous method. The data sets were taken under two different alignments of the probe fibers (the latter alignment, Figure 3.2, was optimized to obtain greater signal strength). The peak intensities (point labeled B in Figure 4.1) for the first alignment ranged from approximately 1900 counts to 3200 counts at 90°F. The peak intensities for the second alignment ranged from approximately 3700 counts to 5800 counts at 90°F. Despite the large differences in overall signal strength, the gamma method predicted accurate values for the viscosities. The mean of the absolute value of the accuacies was 3.1%.

Table 5. 2 Results of ratio method to determine viscosity at 90°F and 110°F

Sample	Gamma 90°F	Viscosity (cs) 90°F	Measured Viscosity (cs) 90°F	Gamma 110°F	Viscosity (cs) 110°F	Measured Viscosity (cs) 110°F
new	0.8104	101.49	97.79 ± 0.61	0.8186	58.20	56.51 ± 0.36
5	0.7451	101.32	90.55 ± 0.57	0.7592	58.02	53.00 ± 0.34
6	0.8325	98.71	100.21 ±0.62	0.8330	56.39	57.36 ± 0.37
7	0.8320	97.15	100.16 ± 0.62	0.8360	55.55	57.53 ± 0.37
8	0.7332	100.01	89.23 ± 0.56	0.7448	57.18	52.15 ± 0.34
9	0.7982	95.60	96.42 ± 0.60	0.8046	54.73	55.68 ± 0.36
10	0.8551	99.91	102.71 ± 0.64	0.8571	56.96	58.79 ± 0.37
11	0.7990	93.61	97.18 ± 0.60	0.7912	53.85	54.92 ± 0.35
12	0.8036	96.76	97.28 ± 0.60	0.8035	55.35	55.62 ± 0.36

Table 5. 3 Results of ratio method to determine viscosity at 140°F

Sample	Gamma 140°F	Viscosity (cs) 140°F	Measured Viscosity (cs) 140°F
new	0.8327	29.04	28.97 ± 0.23
5	0.7504	29.1	27.69 ± 0.22
6	0.8445	28.32	29.54 ± 0.24
7	0.8474	27.96	29.61 ± 0.24
8	0.7496	28.84	27.22 ± 0.22
9	0.8286	27.55	29.65 ± 0.23
10	0.8702	28.56	30.16 ± 0.24
11	0.7954	27.18	28.34 ± 0.23
12	0.8334	27.92	29.27 ± 0.23

To make the gamma method applicable to temperatures other than the three previously discussed, the curve fits of the viscosity versus gamma ratio graphs were used to determine the correlation at any temperature between 90°F and 140°F. The slopes and y-axis intercepts from Figures 4.12 -4.14 (the gamma ratio vs. viscosity graphs) were plotted against temperature. These are shown in Figures 5.1 and 5.2. These curves were then used within the program subroutine Vis_Gamma to determine the correlation equation between viscosity and the gamma ratio at any temperature for which the spectrum could be collected (90°F to 140°F).

To test the accuracy of this method, the program was used to determine the viscosity of the oil samples at 100°F and 120°F (the spectra were collected for these temperatures when the data was collected at 90°F, 110°F and 140°F). Table 5.4 shows the results.

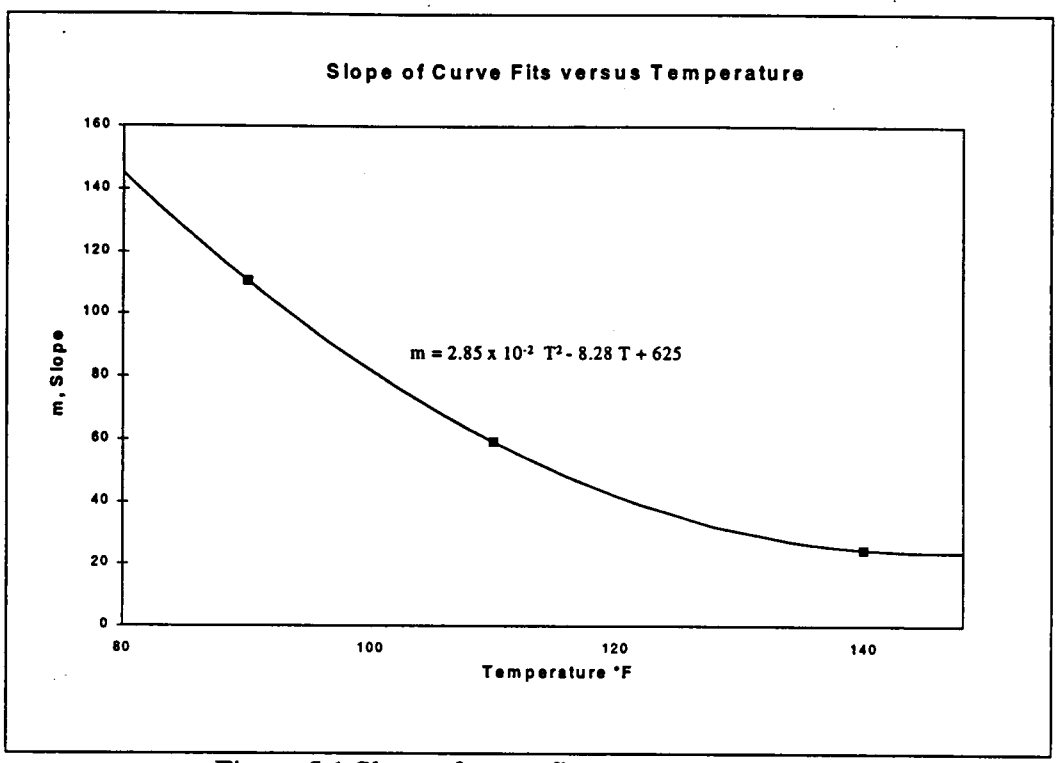


Figure 5.1 Slope of curve fits versus temperature

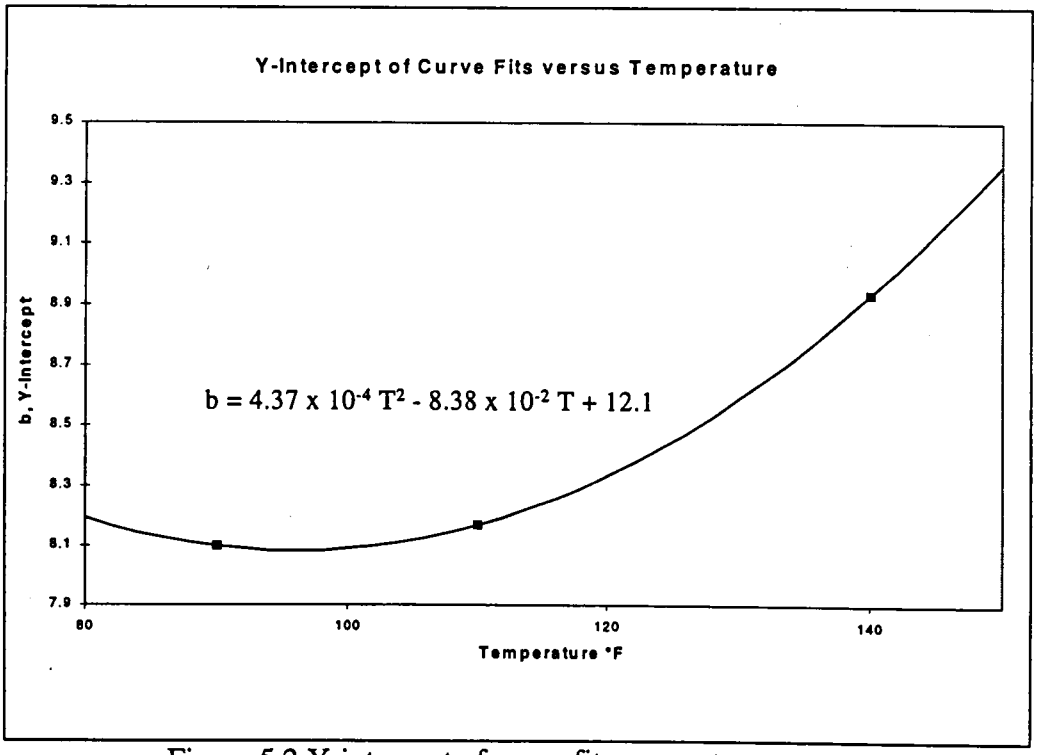


Figure 5.2 Y-intercept of curve fits versus temperature

Table 5. 4 Results of gamma method to determine viscosity at 100°F and 120°F

Sample	Gamma 100°F	Viscosity (cs) 100°F	Measured Viscosity (cs) 100°F	Accuracy	Gamma 120°F	Viscosity (cs) 120°F	Measured Viscosity (cs) 120°F	Accuracy
new	0.8183	77.46	75.21	-2.9	0.8266	43.71	42.89	-1.9
1	0.8176	76.89	75.14	-2.3	0.8240	43.08	42.78	-0.70
2	0.8692	79.56	79.36	-0.25	0.8625	44.30	44.39	-0.20
3	0.7952	58.10	73.30	+26	0.8040	33.79	41.88	+24
4	0.8007	58.10	73.17	+26	0.8021	33.79	41.86	+24
5	0.7581	77.27	70.25	-9.1	0.7549	43.58	39.89	-8.5
6	0.8386	75.19	76.86	+2.2	0.8452	42.31	43.67	+3.2
7	0.8190	74.03	75.24	+1.6	0.8420	41.71	43.53	+4.4
8	0.7354	76.20	68.39	-10.3	0.7444	42.95	39.45	-8.1
9	0.7983	72.89	73.55	+0.91	0.8038	41.12	41.94	+2.0
10	0.8445	76.03	77.34	+1.7	0.8623	42.69	44.38	+4.0
11	0.7906	71.41	72.73	+1.8	0.7943	40.44	41.54	+2.7
12	0.8055	73.79	74.13	+0.46	0.8081	41.63	42.11	+1.2

The actual viscosities reported in the table were taken from the fuels laboratory data. Excluding samples three and four that had high levels of zinc, when the gamma ratio remains above 0.7600 the absolute value of the percent errors ranges from 0.25% to 4.4%. However, when gamma drops below 0.7600 the absolute value of the percent errors ranges from 8.1% to 10.3%. The samples for which the ratio is below 0.7600 had high levels of copper. Therefore, gamma appears to be a good indicator of oil quality. If gamma is above 0.7600, the program can determine the viscosity with good accuracy. If

gamma is below 0.7600, the program can produce an alert that the oil quality has degraded in some manner and more extensive analysis is necessary.

This method of applying the equations to other temperatures could also be applied to the signal strength versus viscosity data. The equations for the slope and y-intercept for those curves would respectively be:

$$m = 5.85 \times 10^{-6} T^2 - 16.0^{-3} \times 10T + 0.144 \qquad \text{Equation 5.1}$$

$$b = 1.99 \times 10^{-2} T^2 - 3.66T + 300 \qquad \text{Equation 5.2}$$

where T is the temperature (in °F).

VI. Conclusion and suggestions for future research

Ultraviolet fluorimetry is an effective technique for *in situ* monitoring of the viscosity of the heavy to medium weight lubricating oil studied here. Two monitoring techniques have been proposed and tested in a laboratory setting. Actual usage conditions were simulated by stirring and heating the oil over the temperature range nominally experienced. The first technique consisted of measuring the fluorescence signal strength at 420 nm. The second technique measured the gamma factor, defined in Section IV.B. The methods exploited empirically determined relationships developed from an initial set of oil samples. The accuracy of both methods is compromised, however, by the presence of high levels of two wear metals, zinc and copper, which typically occur. When contaminant levels remain low, both methods are accurate. Recognition of high contaminant levels of zinc and copper was possible by proper analysis of the spectrum. For zinc, measuring the maximum signal strength and comparing that value to the peak fluorescence signal strength of a new sample indicated excessive levels. Further, a low gamma ratio was seen to indicate high levels of copper.

The ability to recognize high contaminant levels was developed to over come difficulties in determining viscosity. It could however, be implemented as an additional test to determine oil quality. If wear metal contaminants become unacceptably high, the oil quality would be adversely affected. This test could potentially be as important as testing of the viscosity.

Because the system employs fiber optic cables, which form a small probe in addition to the required temperature probe, remote sensing is possible for this process.

When implemented as a probe, the fibers only require a small depth of oil. Therefore, the number of regions of a machine in which the fibers could be used is large. Further, the fibers allow for the remainder of the apparatus to remain at a large distance away from possibly hostile environments.

For future work, both methods should be applied to other types of oils and to samples that exhibit larger variations in viscosity at single temperatures. Correlation of the signal strength changes at one wavelength to viscosity has already been demonstrated by Keller and Saba [7] for diluted samples of turbine engine lubricants. Comparing the gamma ratio to viscosity also has potential for application to other oil types. Burlamacchi *et al* [13] used a 337.1 nanometer laser excitation source to study five different types of crude oil. They reported that all five spectra consisted of the same basic shape, which was the same shape as reported here. The use of pulsed lasers at a specific wavelength (at least an order of magnitude reduced bandwidth in excitation compared to the source used here), such as nitrogen or excimer laser excitation, may give an improved gamma ratio due to selective excitation; the minimum between the peaks, C, should have better definition. This work demonstrates the feasibility of accomplishing the same task without sample dilution, hence enabling *in situ* monitoring possibilities.

REFERENCES

References

1. Stuart, A. D. *et al* "Spectroscopic Measurements of Used Lubricating Oil Quality," Applied Spectroscopy Volume 43, Number 1, pp 55-60, 1989.

2. Bakker, J. de Christopher and Peter M. Fredericks. "Determination of Petroleum Properties by Fiber-Optic Fourier Transform Raman Spectroscopy and Partial Least-Squares Analysis," Applied Spectroscopy Volume 49, Number 12, pp 1766-1770, 1995.

3. Cooper, John B. *et al.* "Remote Fiber-Optic Raman Analysis of Xylene Isomers in Mock Petroleum Fuels Using a Low-Cost Dispersive Instrument and Partial Least-Squares Regression Analysis," Applied Spectroscopy Volume 49, Number 5, pp-586-592, 1995.

4. Goetsch, John G. Jr. "Need to measure viscosity? Determine refractive index instead," *Int*ech pp 40-44, August 1997.

5. Downare, Taggart D. and Oliver C. Mullins. "Visible and Near-Infrared Fluorescence of Crude Oils," Applied Spectroscopy Volume 49, Number 6, pp 754-764, June 1995.

6. Viñas, M. Hernández *et al.* "Fluorescence sensor as an engine oil quality indicator," SPIE Volume 1648 Fiber Optic Medical and Fluorescent Sensors and Application pp 238-247, 1992.

7. Keller, Michael A. and Costandy S. Saba. "Monitoring of Polyphenyl Ether Lubricants Using Fluorescence Spectroscopy," Applied Spectroscopy Volume 44, Number 2, pp 266-268, 1990.

8. Bastow, Trevor *et al.* "Ultraviolet Spectroscopy for the Analysis of Oil-in-Water Effluent Using Isopropanol as Co-solvent," Applied Spectroscopy Volume 51, Number 3, pp 318-322, 1997

9. Stallard, Brian, R. *et al.* "Near-IR Reflectance Spectroscopy for the Determination of Motor Oil Contamination in Sancy Loam," Applied Spectroscopy Volume 50, Number 3, 1996, pp. 334 – 338.

10. Friesen, Waldemar I. "Qualitative Analysis of Oil Sand Slurries Using On-Line NIR Spectroscopy," Applied Spectroscopy Volume 50, Number 12, 1996, pp. 1535 – 1540.

11. Ralston, Corie Y. *et al.* "Quantum Yields of Crude Oils," Applied Spectroscopy Volume 50, Number 12, 1996, pp. 1563 - 1568.

12. Stellaman, Christopher M. "A Fluorescence Based Fiber-Optic Oil Viscosity Monitor," Final Report for Graduate Research Program AEDC, August 1995.

13. Burlamacchi, Pio *et al.* "Performance evaluation of UV sources for lidar fluorosensing of oil films," Applied Optics Volume 22, Number 1,pp 48-53 January 1983.

14. Kung, R.T.V. and I. Itzkan. "Absolute oil fluorescence conversion efficiency," Applied Optics Volume 15, Number 2, pp. 409-415, February 1976.

15. Hoge, F. E. and R.N. Swift. "Experimental feasibility of the airborne measurement of absolute oil fluorescence spectral conversion efficiency," Applied Optics Volume 22, Number 1, pp. 37-46, January 1983.

16. "Professional Course, Viscosity - Part 1", Measurement and Control Volume 28 Number 166 pp. 117 September 1994.

17. Parker, Sybil P. editor. McGraw-Hill Encyclopedia of Physics, 2nd edition. McGraw-Hill, Inc.: New York, 1993, pp. 1509-1510.

18. Hirschfelder, J.O. *et al.* Molecular Theory of Gases and Liquids. John Wiley and Sons Inc.: New York 1954, pp. 625 - 630.

19. Stephan, K. and K. Lucas. Viscosity of Dense Fluids. Plenum Press, New York: 1979, pp. 10-11.

20. Mataga, Noboru and Tanekazu Kubota. Molecular Interactions and Electronic Spectra. Marcel Dekker Inc.: New York, 1970.

21. Berlman, Isadore B. Handbook of Fluorescence Spectra of Aromatic Molecules, 2nd edition. Academic Press: New York, 1971. pp. 330.

22. Graybeal, Jack D. Molecular Spectroscopy, McGraw-Hill Book Company: New York, 1988. pp. 632-633.

23. Tissot, B.P. and D.H. Welte Petroleum Formation and Occurrence, Springer-Verlag: New York, 1984.

24. Fessenden, Ralph J. and Loan S. Fessenden. Organic Chemistry, Brooks/Cole Publishing Company: Pacific Grove, California, 1990.

25. Januszkiewicz, K.R. *et al.* "UV-Fluorescence Spectroscopic Method for Monitoring Tramp Oil contamination in Hot Rolling Emulsions" Lubrication Engineering, Volume **47**, 6, 448-452, 1991.

26. Boldt, Kenneth and B.R. Hall. Significance of tests for Petroleum Products, American Society for testing and Material: Philadelphia, Pennsylvania, 1977. pp. 203

27. Communication with technical support at Mobil Corporation.

28. Parigger, Christian *et al.* "Exciplex liquid-phase thermometer using time-resolved laser-induced fluorescence" Optics Letters Volume 23, Number 1, pp. 76-78, January 1998.

29. Murray, A.M. and L. A. Melton. "Fluorescence methods for determination of temperature in fuel sprays" Applied Optics Volume 24, Number 17, pp. 2783-2787, September 1985.

APPENDICES

Appendix A. AEDC Fuels Laboratory Results

The following is the compete list of chemicals for which the AEDC chemistry lab tested the Mobil heavy to medium weight oil to determine content. All of these were found to be below detectable levels.

Dichlorodifluoromethane

Chloromethane

Vinyl Chloride

Bromomethane

Chloroethane

Trichlorofluoromethane

1,1-Dichloroethane

Acetone

Trichlorotrifluoroethane

Methylene Chloride

trans-1,2-Dichloroethene

1,1- Dichloroethane

cis,1,2- Dichloroethane

2,2-Dichloropropane

2-Butanone

Bromochloromethane

Chloroform

1,1,1,-Trichloroethane

Tetrachloroethene

Dibromochloromethane

1,2-Dibromoethane

Chlorobenzene

1,1,1,2-Tetrachloroethane

Ethylbenzene

m,p-Xylenes

Styrene

Bromoform

Isopropylbenzene

1,1,2,2-Tetrachloroethane

Bromobenzene

1,2,3-Trichloropropane

n-Propylbenzene

2-Chlorotoluene

1,3,5-Trimethylbenzene

4-Chlorotoluene

tert-Butylbenzene

1,1-Dichloropropene

Carbon Tetrachloride

1,2-Dichloroethane

Benzene

Trichloroethene

1,2 Dichloropropane

Dibromomethane

Bromodichloromethane

trans,-1,3-Dichloropropene

1,1,2-Trichloroethane

1,3-Dichloropropane

Toluene

1,2,4-Trimethylbenzene

sec- Butylbenzene

1,3-Dichlorobenzene

p-Isopropyltoluene

1,4- Dichlorobenzene

n-Butylbenzene

1,2- Dichlorobenzene

1,2,4-Trichlorobenzene

Hexachlorobutadiene

Naphthalene

1,2,3- Trichlorobenzene

cis-1,3-Dichloropropene

Appendix B. Discussion of Naphthalene

The following figures provided background information on the molecule naphthalene.

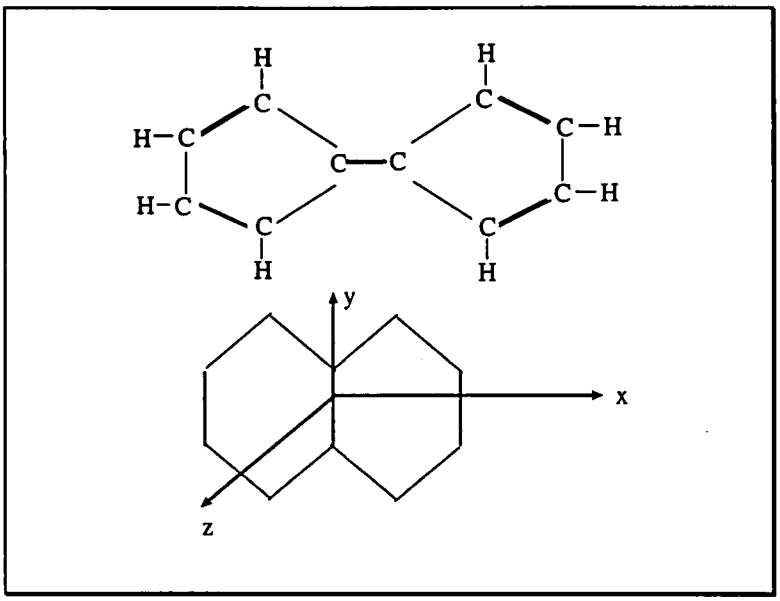


Figure B.1 Structure of Naphthalene

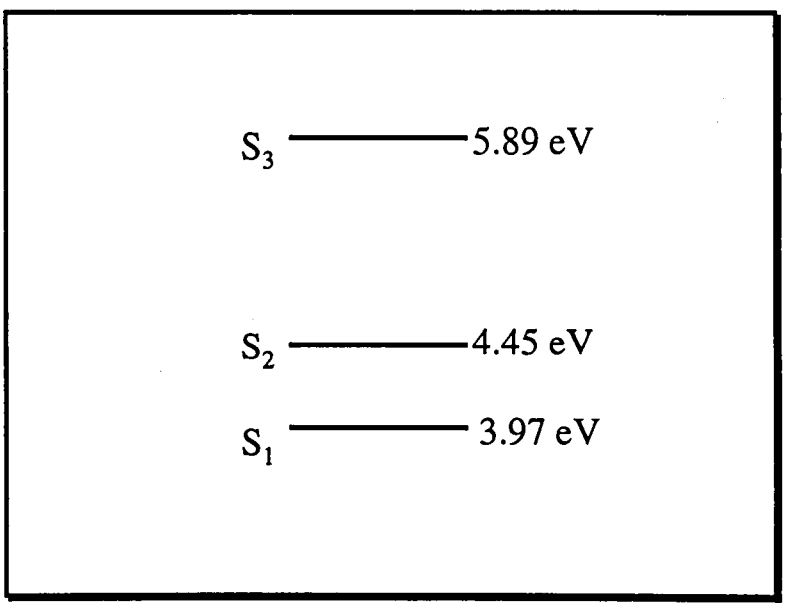


Figure B.2 Electronic energy levels of naphthalene

Appendix C. AEDC Precision Measurement Equipment Laboratory Results

The following graphs display the results of the CCD detector response, the transmission of the bandpass filter and the irradiance of the 75 Watt Xenon arc lamp.

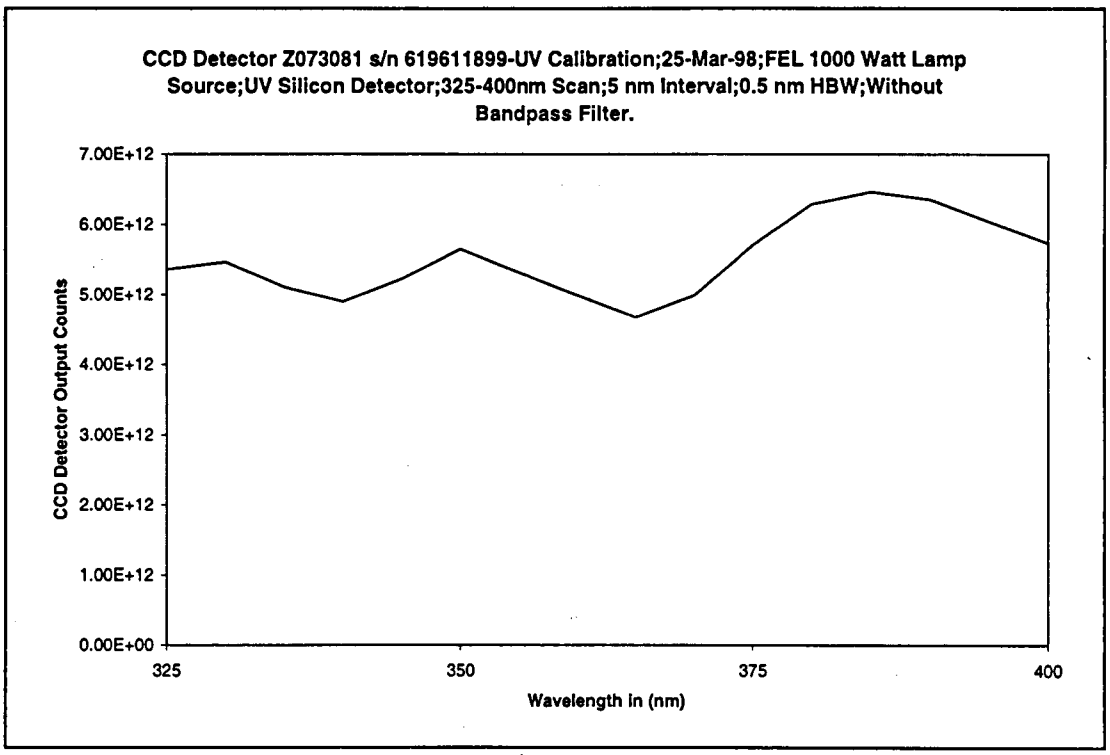


Figure C.1 CCD Detector Response

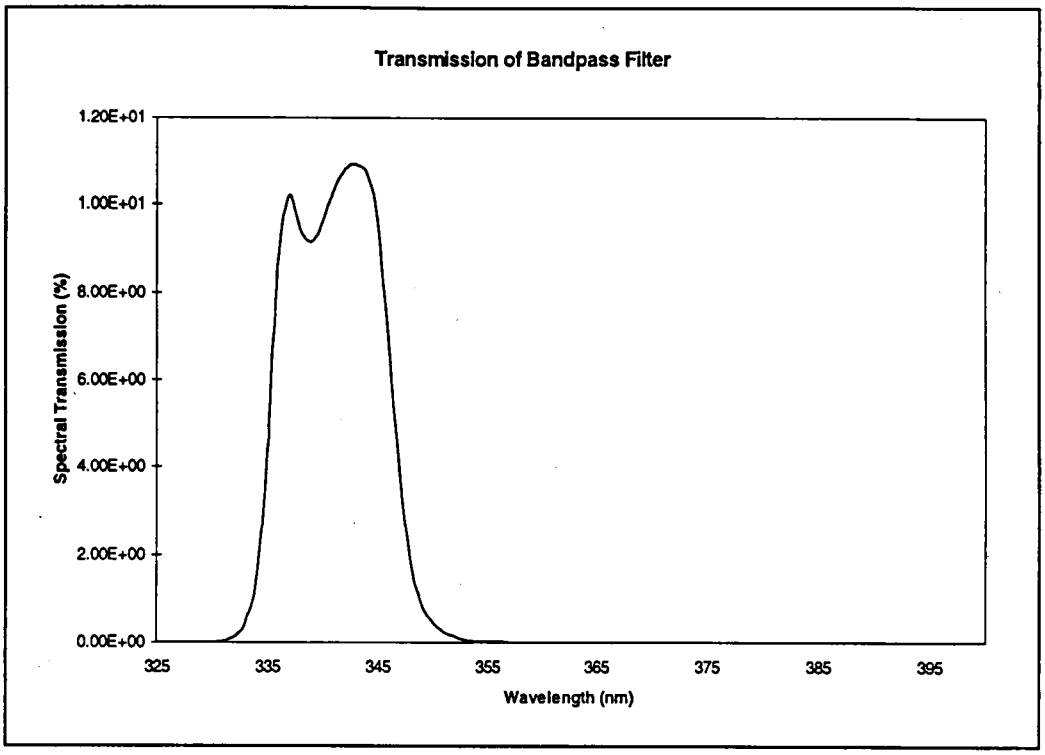


Figure C.2 Transmission of Bandpass Filter

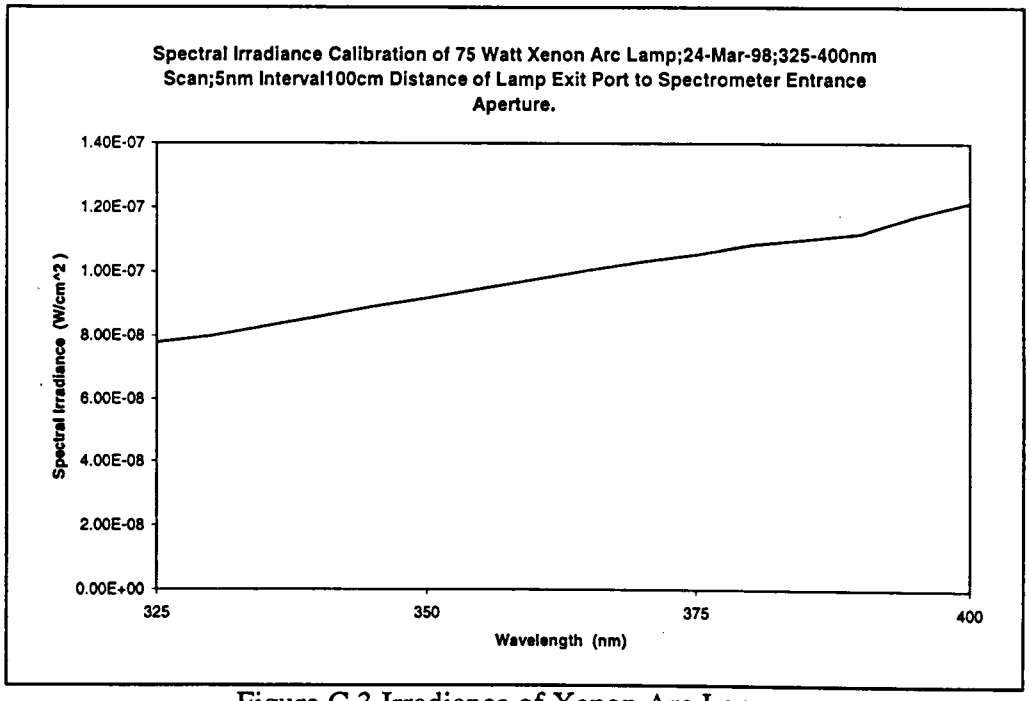


Figure C.3 Irradiance of Xenon Arc Lamp

Appendix D. Analysis.for

In this appendix, the program listing of the Microsoft Fortran program written for this project is shown. This program requires the filename under which the spectrum is saved and the temperature at which the spectrum was collected. The program uses those measured quantities to calculate the viscosity of the oil from the curve fit equations given in Figures 4.9 – 5.2.

Program Spectra_Analysis

```
c Last updated: 12/1/97
c Program to compute the viscosity of an oil sample from
c its fluorescence spectrum. The program is designed to accepted
c the data as it is saved in ASCII format in the SBIG CCD camera.
c In the program intensity is used for signal strength.
c
c  Defined variables:
c
c  totpix:the total number of pixels across the CCD array
c  loca: pixel number of the location of the first peak maximum
c  locb: pixel number of the location of the second peak maximum
c  locc: pixel number of the location of the minimum between
c       loca and locb
c  fstpk: intensity of the first peak
c  sndpk: intensity of the second peak
c  intpix: intensity of pixel #110 corresponding to a wavelength
c        of 420 nanometers
c
c  Input variables:
c
c  t: temperature of oil at which the spectrum was collected
c
c  Other required input:
c
c  The filename under which the spectrum is saved
c
c  Calculated variables:
```

```
c
c   gamma: The ratio of the intensity at locc/locb
c   viscosity:viscosity of oil calculated from comparison of
c          fluorescence at 420 nanometers
c   vis_b:viscosity of oil calculated for the gamma ratio
c
c**********************************************************************
      integer n,l,m,totpix,loca,locb,fstpk,sndpk,t,visc,intpix
      integer min,locc, vis_b
      real*4 gamma
      Parameter (totpix=375.0)
      integer pixel(totpix),intensity(totpix)
      n=1
      open(1,file='//data//', status ='old', iostat=ios)
      do while (n.le.totpix)
        read(1,*,iostat=ios) pixel(n),intensity(n)
        n=n+1
      enddo
      print*, 'Intensity @ 420nm = ',intensity(110)
      intpix=intensity(110)
      call maxpix(m,l,intensity,fstpk,sndpk,loca,locb,min,locc)
      gamma = (sndpk**(-0.9999999))*min
      print*, 'gamma ratio = ',gamma
      print*, 'what is the temperature?'
      read*, t
      call zincwarn(sndpk,t)
      call Viscosity(t,intpix,visc)
      call Vis_Gamma(t,vis_b,gamma)
      end
c**********************************************************************
      Subroutine maxpix(m,l,intensity,fstpk,sndpk,loca,locb,min,locc)
c This subroutine locates the maximum intensity of the first and second
c peaks.  Its also locates the minimum between the peaks.  Its then
c averages the individual values they there first nearest neighbors.
c This was done to reduce the change of noise adversely effecting
c the measurements.
      parameter (totpix=375)
      integer m,l,k,locb, min,locc
      integer loca,fstpk,sndpk,intensity(m)
      m=1
      l=260
      fstpk=intensity(m)
      sndpk=intensity(260)
      loca=1
```

```
      locb=260
      do while (m.le.260)
            if (fstpk.le.intensity(m))then
                  fstpk=intensity(m)
                  loca=m
             else
                  fstpk=fstpk
                  loca=loca
            endif
            m=m+1
      enddo
      do while (l.le.totpix)
            if (sndpk.le.intensity(l))then
                  sndpk=intensity(l)
                  locb=l
            else
                  sndpk=sndpk
                  locb=locb
            endif
            l=l+1
      enddo
      k=loca
      min = fstpk
      locc = loca
      do while (k.le.locb)
            if (min.gt.intensity(k))then
                 min=intensity(k)
                 locc = k
            else
                  min = min
                  locc = locc
            endif
            k=k+1
      enddo
      end
c**********************************************************************
      Subroutine Viscosity(t,intpix,visc)
c This subroutine calculates the viscosity of the oil by substituting
c the intensity of the fluorescence spectrum at 420 nanometers into
c first order polynomial fits of the Intensity vs. Viscosity curves.
c These curves were developed from viscosity measurements done by
c traditional means. This comparison is only available for the three
c temperatures of 90, 110 and 140 degrees Fahrenheit.
      integer t,intpix,visc
```

```
      if (t.eq.90) then
         visc = 0.0168 * intpix + 67.5
      print*,'viscosity from intensity @ 420nm= ',visc,'centi-stokes'
      else if (t.eq.110) then
         visc= 0.00817 * intpix + 42.1
      print*,'viscosity from intensity @ 420nm= ',visc,'centi-stokes'
      else if (t.eq.140) then
         visc = 0.00402 *intpix + 21.9
      print*,'viscosity from intensity @ 420nm= ',visc,'centi-stokes'
      else
         print*, 'Viscosity calculation only available'
         print*, 'for temperatures of 90,110, & 140 degrees'
         print*, 'from intensity @ 420nm subroutine.'
      end if
      end
c**********************************************************************
      Subroutine zincwarn (sndpk,t)
c This subroutine compares the value of the maximum intensity of the
c analyzed spectrum to the maximum intensity of the new oil spectrum.
c If the value is at least 50 counts higher than that of the new oil,
c the program returns a warning.  If the value is lower, no warning
c is given.
      integer t, sndpk
      real znpk
      znpk =  0.064*(t*t) - 34.3*t + 7304
      znpk = znpk + 50
      if (sndpk.gt.znpk) then
          print*, 'WARNING: Zinc level may be high!'
          print*, 'Viscosity reading may not be accurate.'
      else
          print*, ' Zinc level acceptable'
      endif
      end
c**********************************************************************
      Subroutine Vis_Gamma(t,vis_b,gamma)
c This subroutine uses the gamma ratio to determine the viscosity.
c It is capable of calculation the viscosity at any temperature.
c It should only be considered accurate from 80 to 160 degrees
c Fahrenheit.
      real slope, yint
      integer vis_b,t
      slope = 0.0285*(t**2) - 8.28*t +625
      yint = 0.000437*(t**2) - 0.0838*t +12.1
      vis_b = slope * gamma + yint
```

```
      if (gamma.lt.0.800) then
        print*, 'Warning: viscosity reading may be inaccurate'
        print*, 'High levels of contaminants may exist.'
      print*,'Viscosity from Gamma ratio =     ',vis_b,'centi-stokes'
      else
      print*,'Viscosity from Gamma ratio =     ',vis_b,'centi-stokes'
      endif
      end
c*************************************************************************
```

Vita

Shawn C. Dancik was born in Butler, Pennsylvania January 10, 1974. He attended Bulter Area High School and graduated 15th in his class. In 1992, he enrolled at Wheeling Jesuit College to pursue a Bachelors degree. In 1996, he graduated magna cum laude, receiving a Bachelor of Science degree in both mathematics and physics.

In the fall of 1996, he accepted a graduate research assistantship at the University of Tennessee Space Institute. His research work was conducted at Arnold Engineering Development Center, Arnold Air Force Base, TN. He was awarded the Master of Science degree in Physics in December 1998.